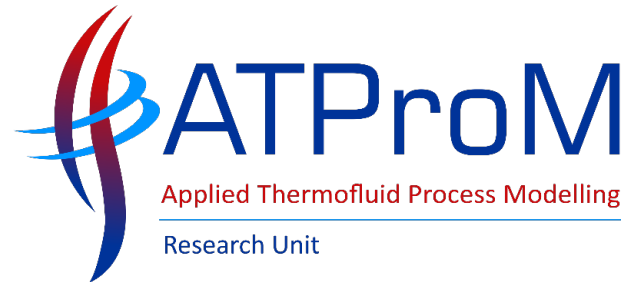


A method to develop centrifugal compressor performance maps for off-design and dynamic simulation studies of sCO₂ cycles



Presented by Colin Francois du Sart (Colin.duSart@uct.ac.za), University of Cape Town
Co-authored by Pieter Rousseau & Ryno Laubscher, Stellenbosch University

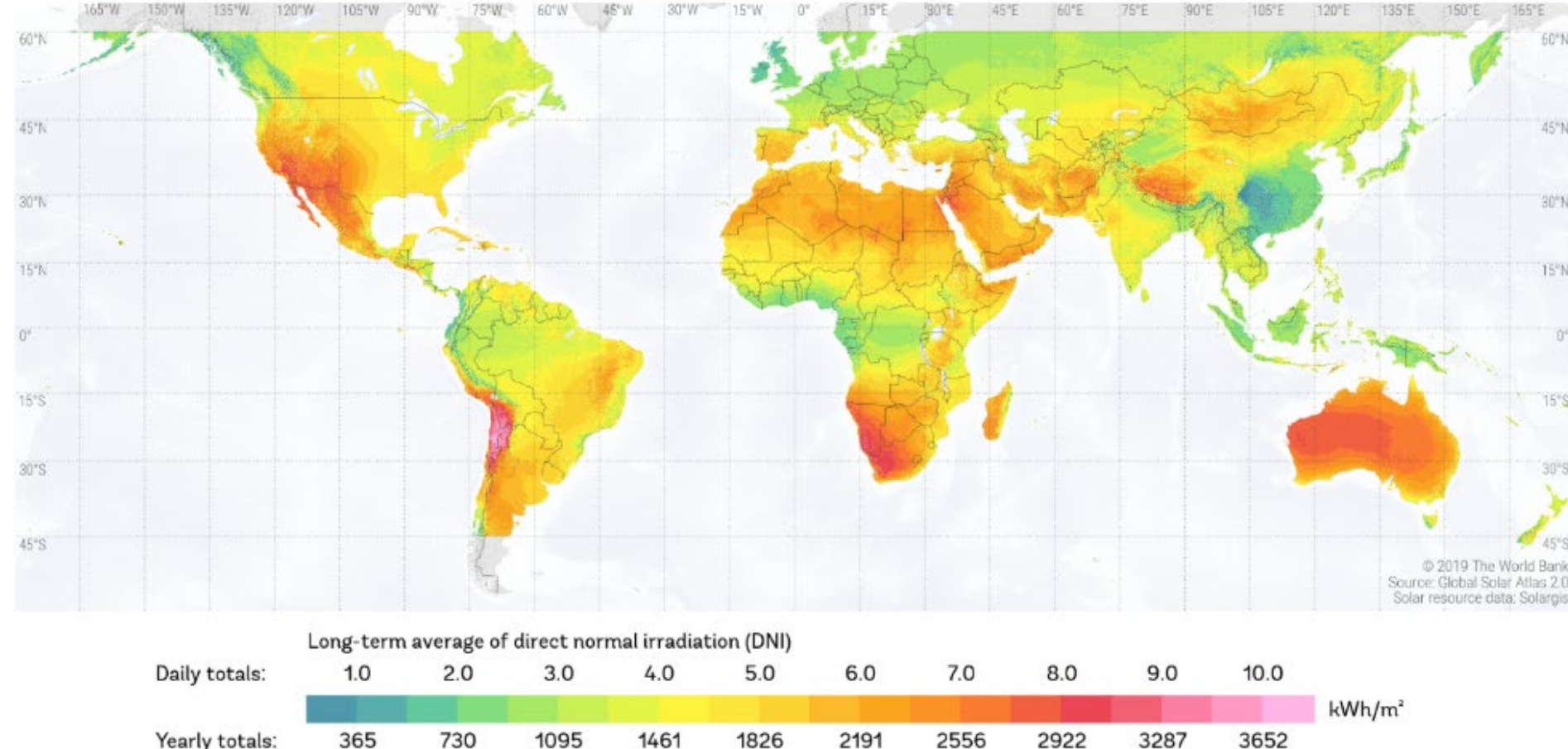
Introduction

SOLAR RESOURCE MAP **DIRECT NORMAL IRRADIATION**

WORLD BANK GROUP

ESMAP

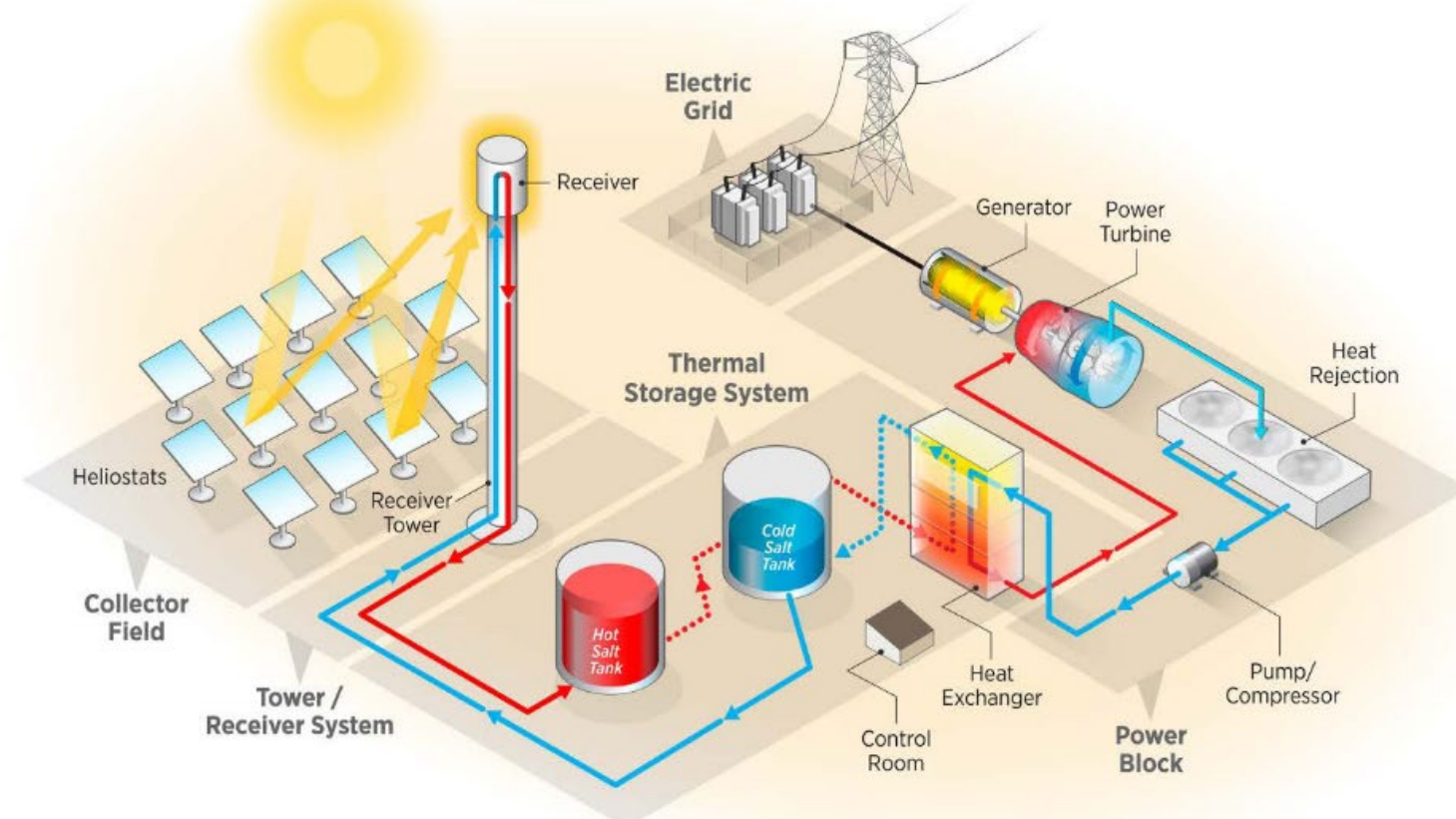
SOLARGIS



This map is published by the World Bank Group, funded by ESMAP, and prepared by Solargis. For more information and terms of use, please visit <http://globalsolaratlas.info>

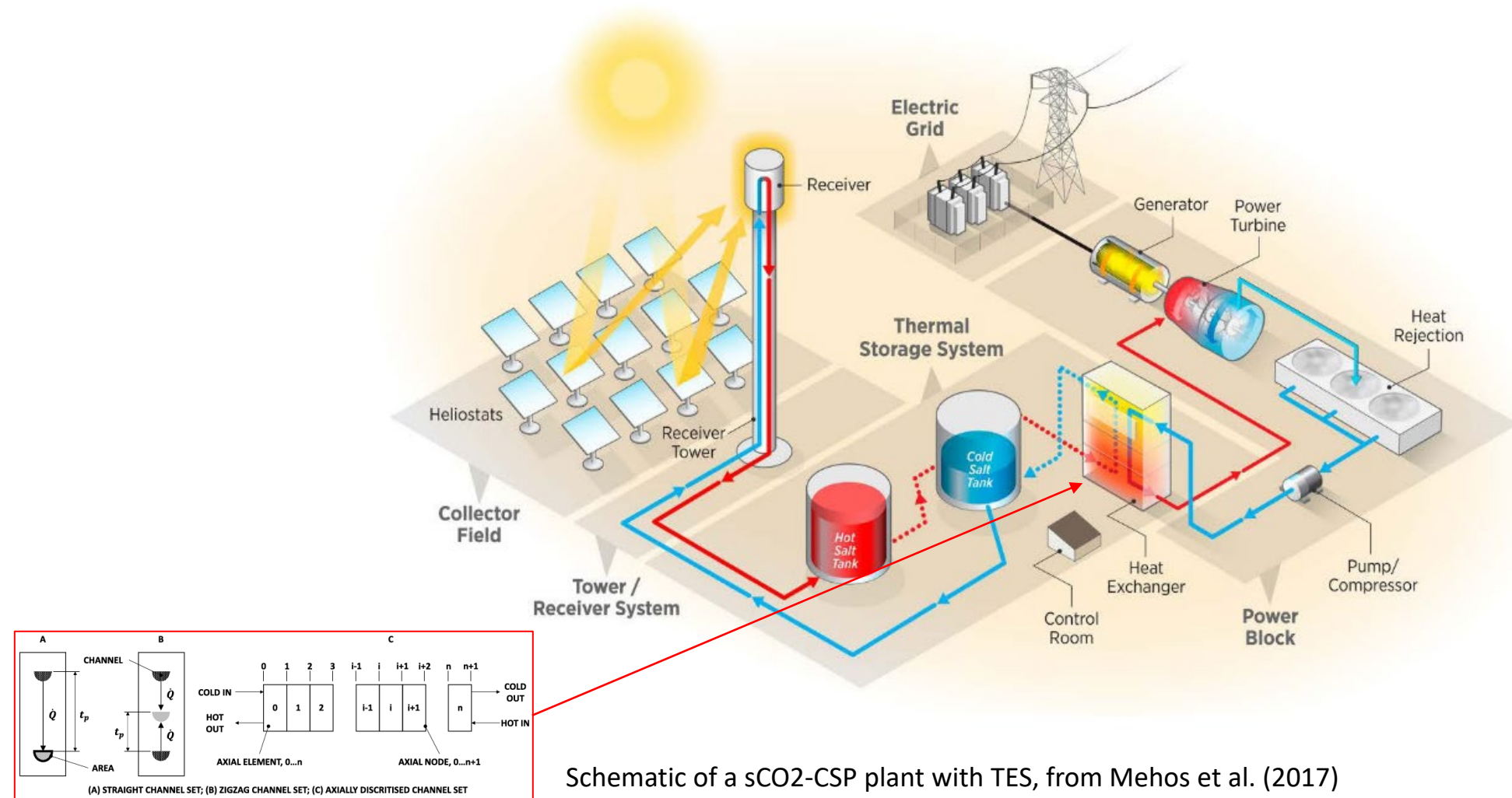
Global direct normal irradiation map, from The World Bank (2019)

Introduction

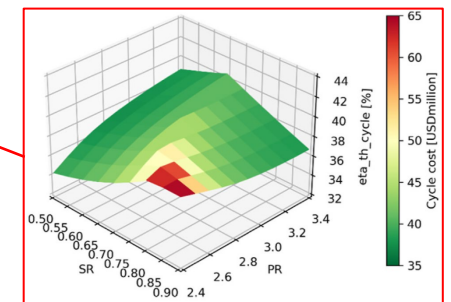
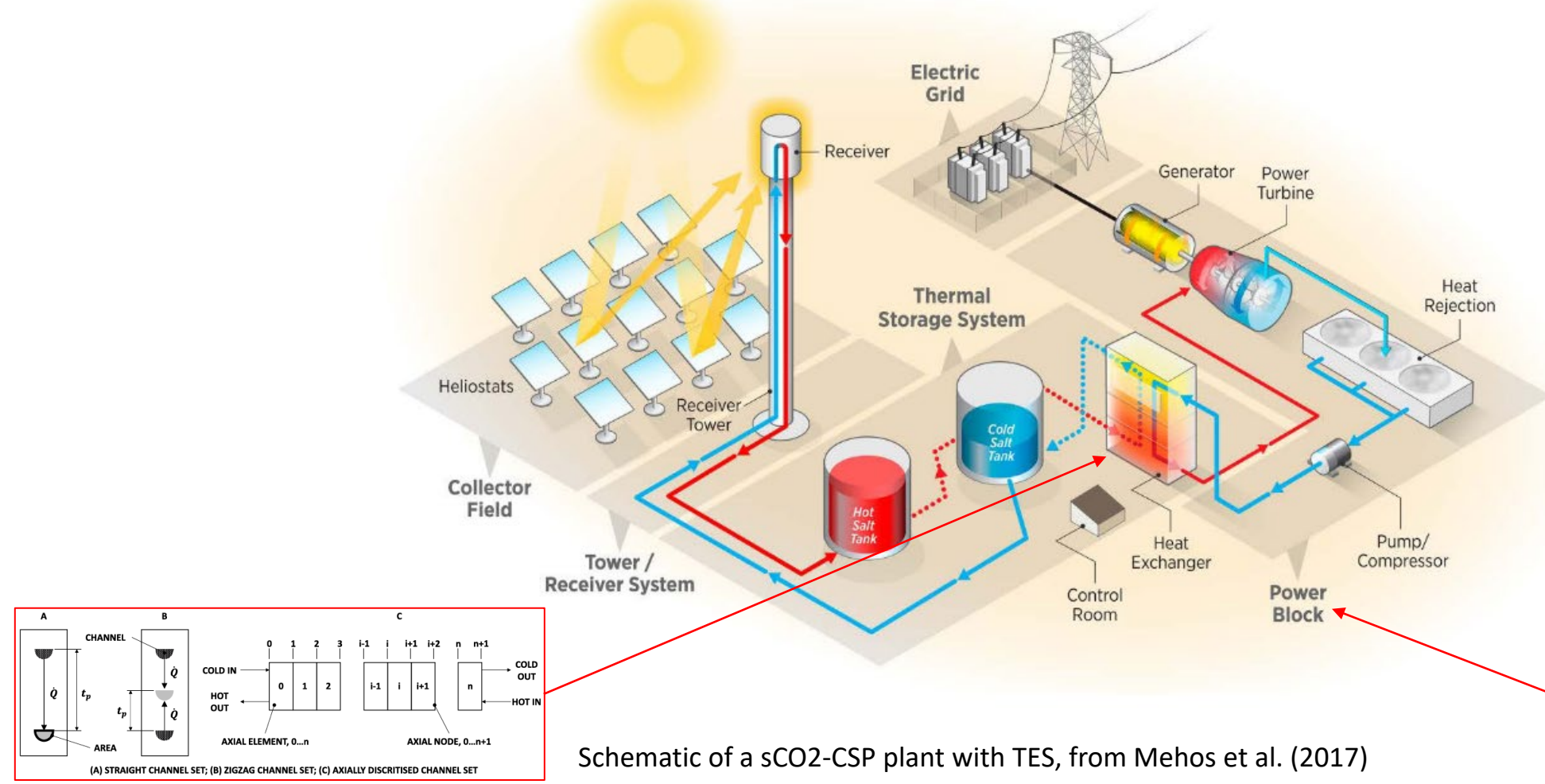


Schematic of a sCO₂-CSP plant with TES, from Mehos et al. (2017)

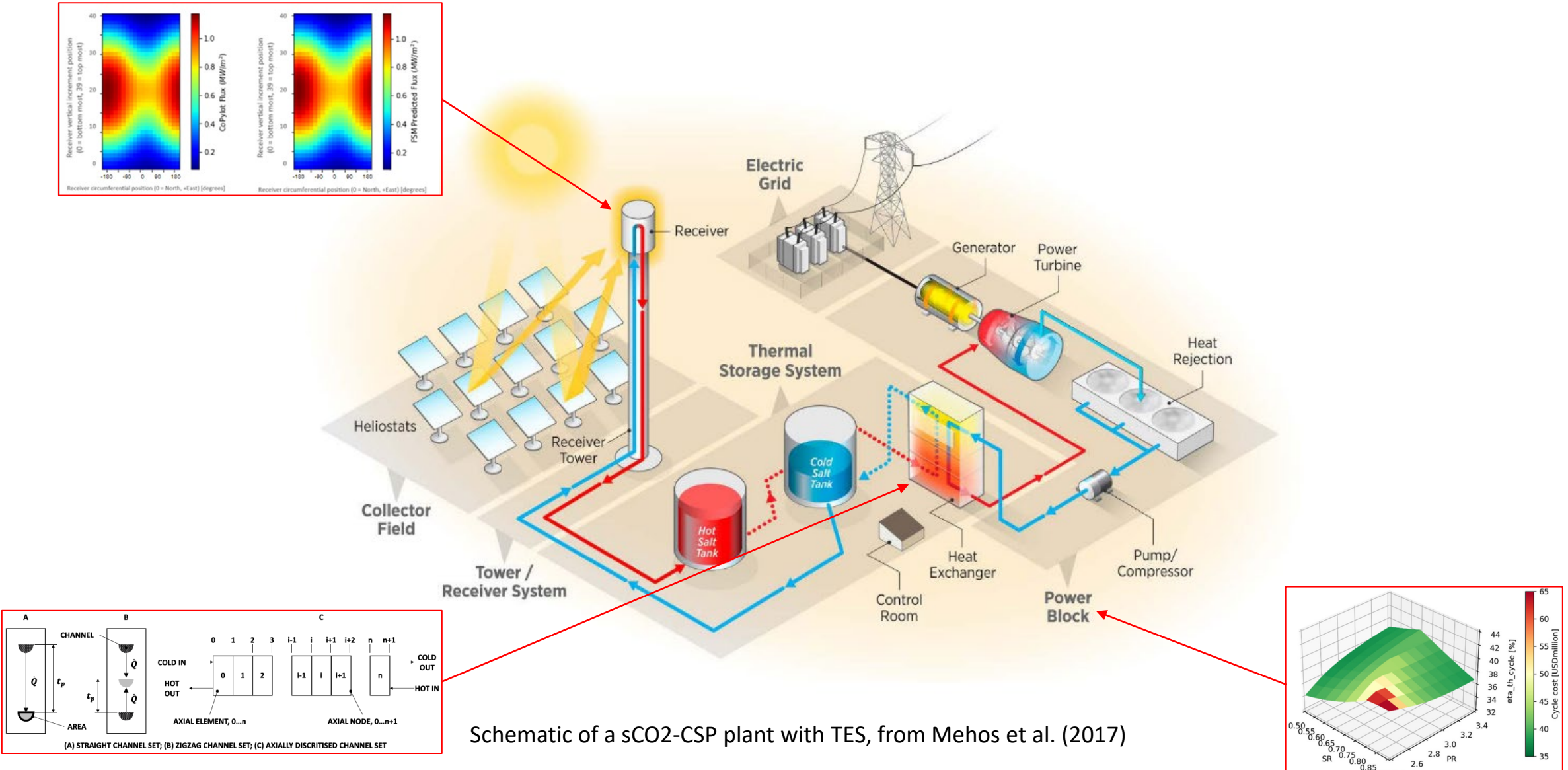
Introduction



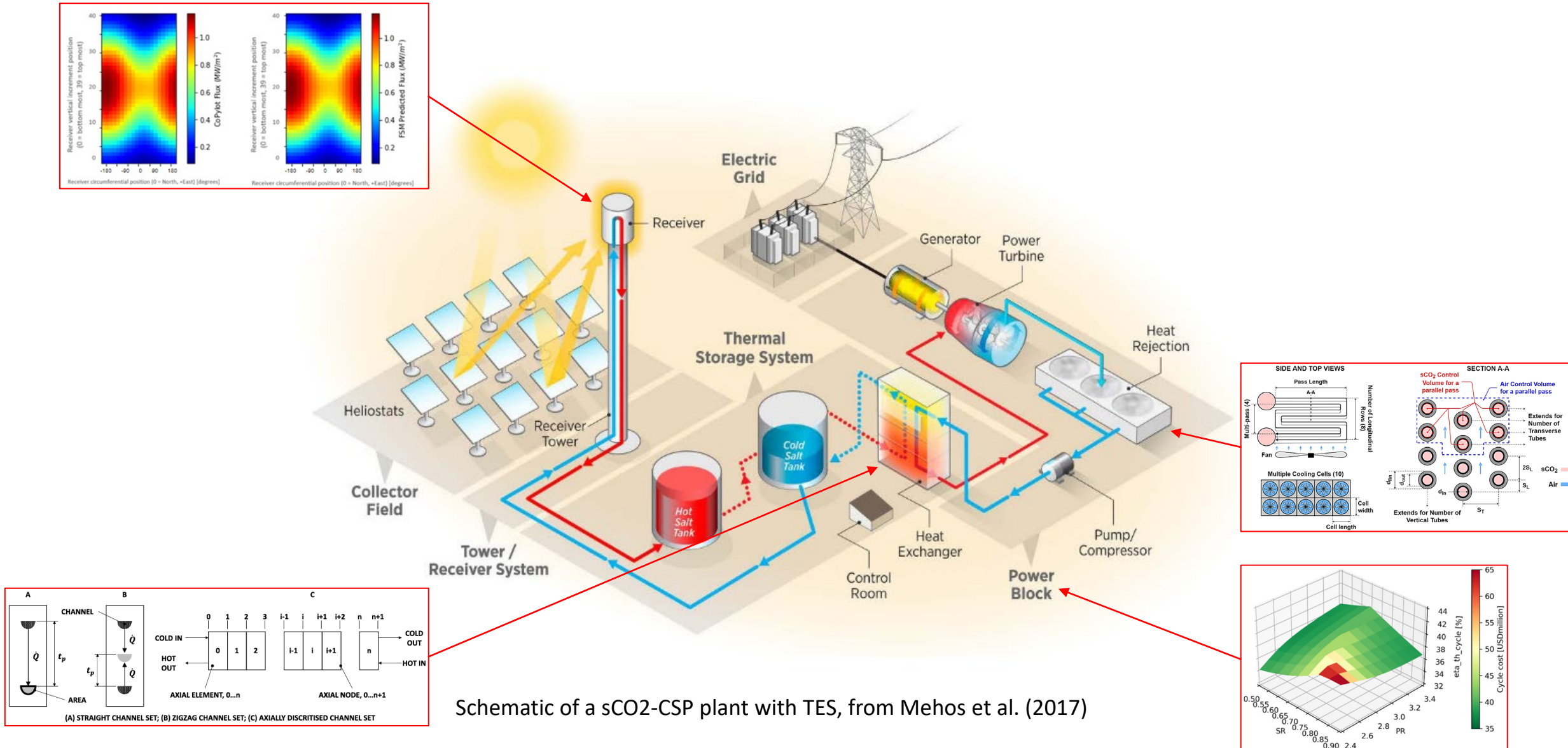
Introduction



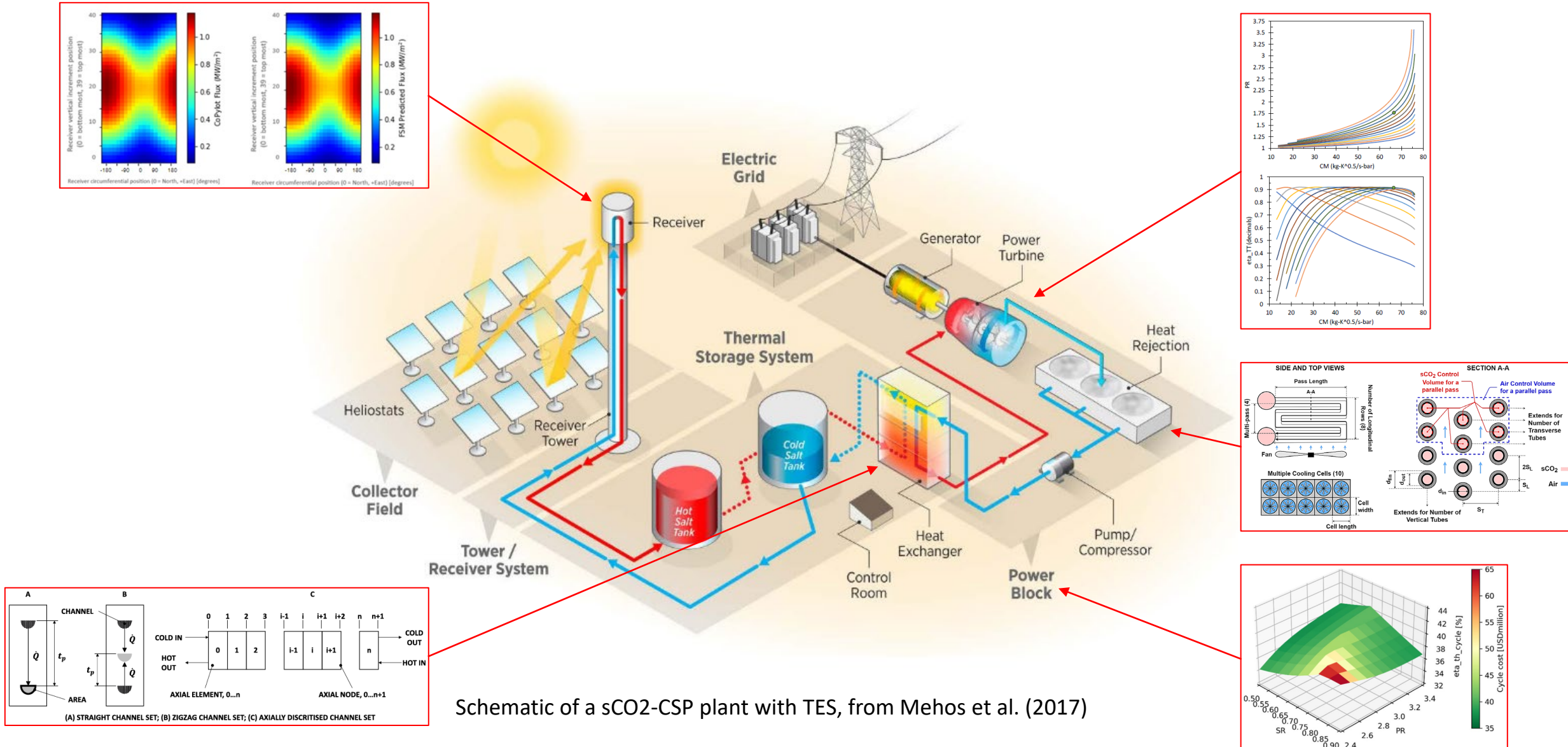
Introduction



Introduction



Introduction



Literature review

		Dostal et al. (2004)	Carstens (2007)	Seidel (2010)	Kulhanek & Dostal (2011a)	Turchi et al. (2013)	Dyreby (2014)	Neises & Turchi (2014)	Padilla et al. (2015)	Osorio et al. (2016)	Binotti et al. (2017)	Luu et al. (2017a)	Luu et al. (2017b)	Neises & Turchi (2019)	Thanganadar et al (2020)	Correa et al (2021)	Yang et al (2023)
Study type	Steady-state	x		x	x	x	x	x						x			
	Quasi-steady		x						x	x	x		x	x	x	x	
	Dynamic		x									x					
Turbomachinery models	Isentropic			x	x	x		x	x	x	x	x	x	x	x	x	
	Dyreby's method/ curve fit						x					x		x	x	x	
	Performance maps by others/ software	x	x														
	Tailor-made design and maps																
	Inertia effects																
Off-design performance, control and simulations	Off-design performance						x								x		
	Off-design control	x												x			
	Daily simulation								x		x	x					
	Annual simulation			x					x				x		x		
	Fast transients		x														

Literature review

		Dostal et al. (2004)	Carstens (2007)	Seidel (2010)	Kulhanek & Dostal (2011a)	Turchi et al. (2013)	Dyreby (2014)	Neises & Turchi (2014)	Padilla et al. (2015)	Osorio et al. (2016)	Binotti et al. (2017)	Luu et al. (2017a)	Luu et al. (2017b)	Neises & Turchi (2019)	Thanganadar et al (2020)	Correa et al (2021)	Yang et al (2023)
Study type	Steady-state	x			x	x	x	x							x		
	Quasi-steady			x						x	x	x		x	x	x	
	Dynamic		x										x				
Turbomachinery models	Isentropic			x	x	x		x	x	x	x	x		x	x		
	Dyreby's method/ curve fit						x						x		x	x	
	Performance maps by others/ software	x	x														
	Tailor-made design and maps																
	Inertia effects																
Off-design performance, control and simulations	Off-design performance						x								x		
	Off-design control	x												x			
	Daily simulation									x		x	x				
	Annual simulation			x						x				x			
	Fast transients		x														

Literature review

		Dostal et al. (2004)	Carstens (2007)	Seidel (2010)	Kulhanek & Dostal (2011a)	Turchi et al. (2013)	Dyreby (2014)	Neises & Turchi (2014)	Padilla et al. (2015)	Osorio et al. (2016)	Binotti et al. (2017)	Luu et al. (2017a)	Luu et al. (2017b)	Neises & Turchi (2019)	Thanganadar et al (2020)	Correa et al (2021)	Yang et al (2023)
Study type	Steady-state	x			x	x	x	x							x		
	Quasi-steady			x					x	x	x			x	x	x	
	Dynamic		x									x					
Turbomachinery models	Isentropic			x	x	x		x	x	x	x	x		x	x		
	Dyreby's method/ curve fit						x						x		x	x	
	Performance maps by others/ software	x	x														
	Tailor-made design and maps																
	Inertia effects																
Off-design performance, control and simulations	Off-design performance						x								x		
	Off-design control	x												x			
	Daily simulation								x		x	x	x				
	Annual simulation			x					x	x				x			
	Fast transients		x														

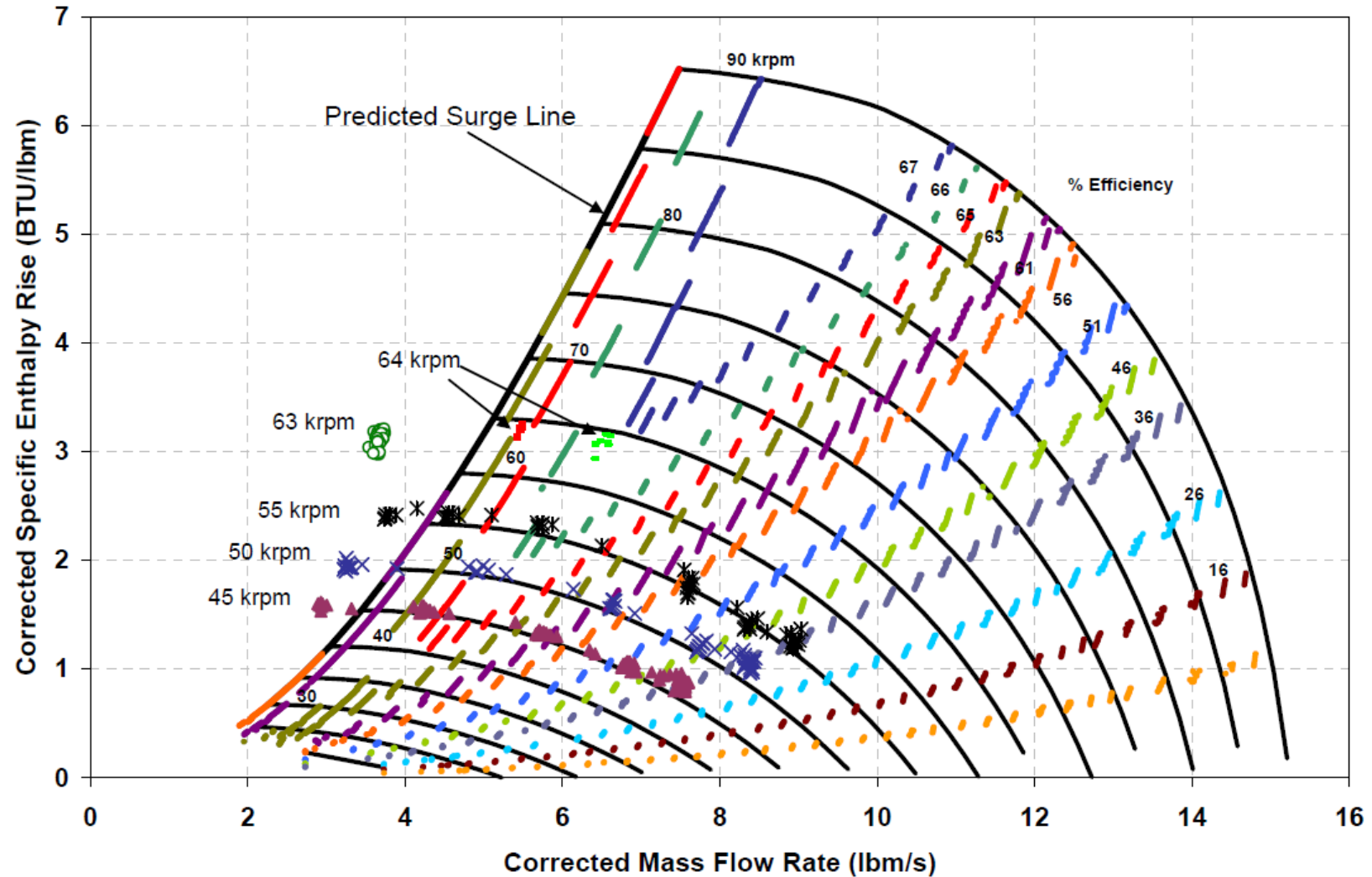
Literature review

		Dostal et al. (2004)	Carstens (2007)	Seidel (2010)	Kulhanek & Dostal (2011a)	Turchi et al. (2013)	Dyreby (2014)	Neises & Turchi (2014)	Padilla et al. (2015)	Osorio et al. (2016)	Binotti et al. (2017)	Luu et al. (2017a)	Luu et al. (2017b)	Neises & Turchi (2019)	Thanganadar et al (2020)	Correa et al (2021)	Yang et al (2023)
Study type	Steady-state	x		x	x	x	x	x							x		
Turbomachinery models	Quasi-steady			x					x	x	x	x	x	x	x	x	
	Dynamic		x									x					
	Isentropic			x	x	x		x	x	x	x	x	x	x	x	x	
	Dyreby's method/ curve fit						x					x		x	x	x	
	Performance maps by others/ software	x	x														
	Tailor-made design and maps																
	Inertia effects																
Off-design performance, control and simulations	Off-design performance						x								x		
	Off-design control	x												x			
	Daily simulation								x		x	x	x				
	Annual simulation			x					x					x			
	Fast transients		x														

Literature review

		Dostal et al. (2004)	Carstens (2007)	Seidel (2010)	Kulhanek & Dostal (2011a)	Turchi et al. (2013)	Dyreby (2014)	Neises & Turchi (2014)	Padilla et al. (2015)	Osorio et al. (2016)	Binotti et al. (2017)	Luu et al. (2017a)	Luu et al. (2017b)	Neises & Turchi (2019)	Thanganadar et al (2020)	Correa et al (2021)	Yang et al (2023)
Study type	Steady-state	x		x	x	x	x	x						x			
Turbomachinery models	Quasi-steady		x						x	x	x		x	x	x	x	
	Dynamic		x									x					
	Isentropic			x	x	x		x	x	x	x		x	x	x	x	
	Dyreby's method/ curve fit						x					x		x	x	x	
	Performance maps by others/ software	x	x														
	Tailor-made design and maps																
	Inertia effects																
Off-design performance, control and simulations	Off-design performance						x								x		
	Off-design control	x												x			
	Daily simulation								x		x	x					
	Annual simulation			x					x				x		x		
	Fast transients		x														

Dyreby's method



SNL compressor performance map, from Wright et al. (2010)

Dyreby's method

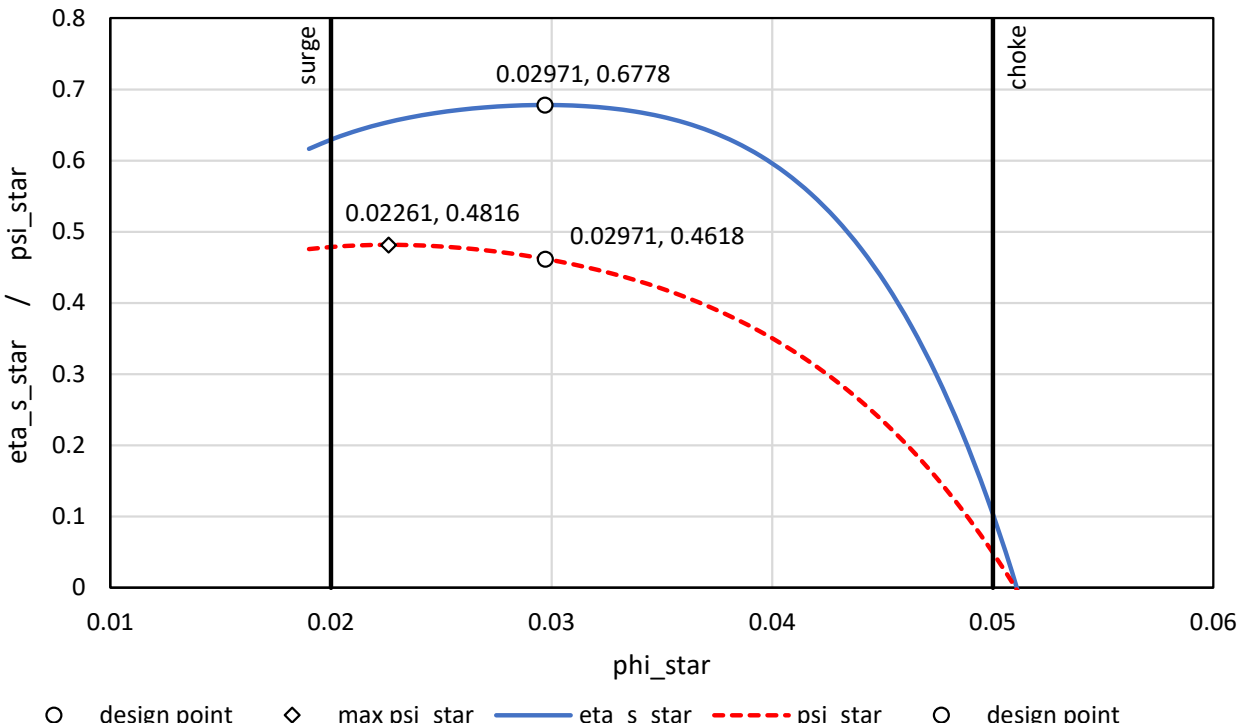
$$\eta^* = -0.7069 + 168.6\phi^* - 8089\phi^{*2} + 182725\phi^{*3} - 1.638e^6\phi^{*4}$$

$$\psi^* = 0.04049 + 54.7\phi^* - 2505\phi^{*2} + 53224\phi^{*3} - 498626\phi^{*4}$$

$$\phi^* = \phi \left(\frac{N}{N_{nom}} \right)^{0.2} = \frac{\dot{m}}{\rho_1 u_2 D_2^2} \left(\frac{N}{N_{nom}} \right)^{0.2}$$

$$\eta^* = \eta \left(\frac{N_{nom}}{N} \right)^{(20\phi^*)^5}$$

$$\psi^* = \psi \left(\frac{N_{nom}}{N} \right)^{(20\phi^*)^3} = \frac{w_{c.s.}}{u_2^2} \left(\frac{N_{nom}}{N} \right)^{(20\phi^*)^3}$$



Head and efficiency correlations, from Dyreby (2014)

KAIST-TMD:

- Private 1D mean-line based tool to size centrifugal compressors and generate performance maps.
- Developed by Lee (2016) for the design of sCO₂ centrifugal compressors.
- Used by collaborators i.e., Cho et al. (2019) and Jeong et al (2020) for compressor-focused studies.

KAIST-TMD:

- Private 1D mean-line based tool to size centrifugal compressors and generate performance maps.
- Developed by Lee (2016) for the design of sCO₂ centrifugal compressors.
- Used by collaborators i.e., Cho et al. (2019) and Jeong et al (2020) for compressor-focused studies.

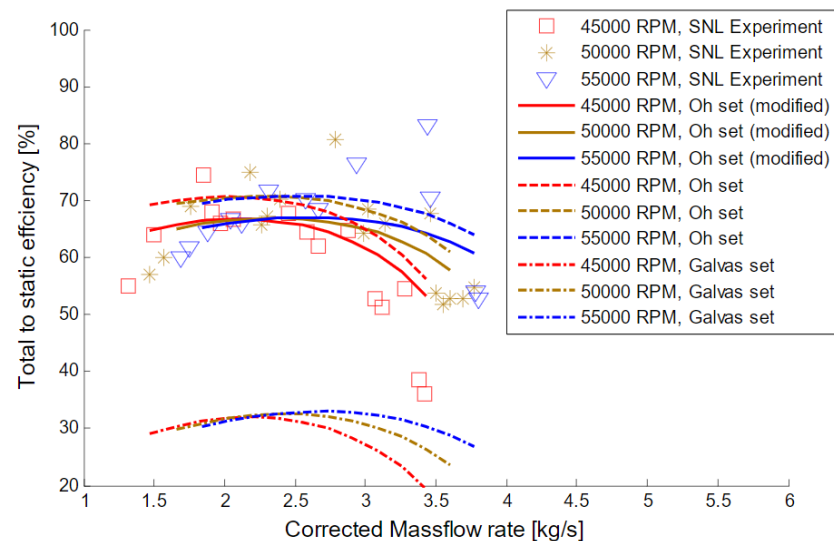
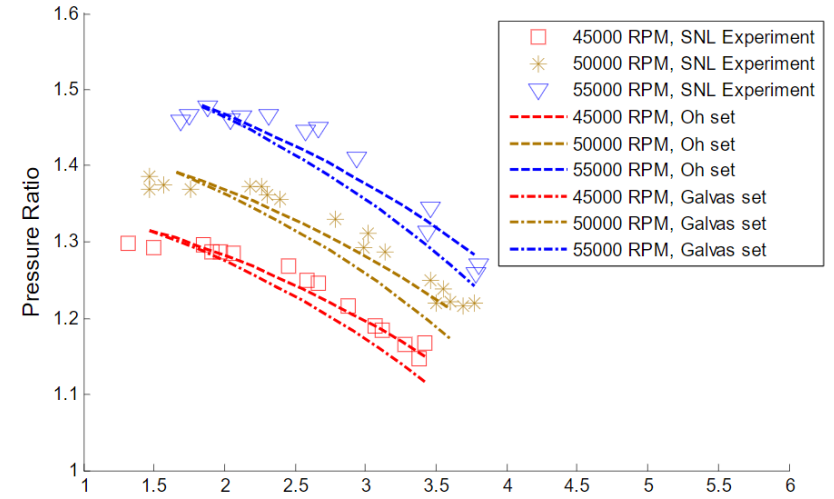
AlFa CCD:

- Private 1D mean-line based tool to size centrifugal compressors and generate performance maps.
- Developed by Ameli et al (2018) for the design of sCO₂ centrifugal compressors.

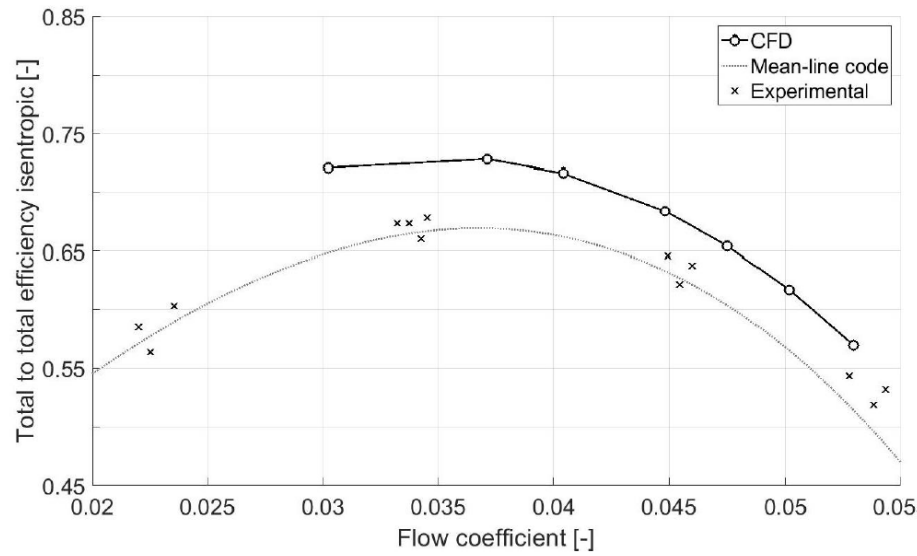
Compared to this work:

- Fewer compressor components considered.
- Models not fully documented.
- Different correlation sets applied.
- Verification results leave room for improvement.

1D mean-line codes

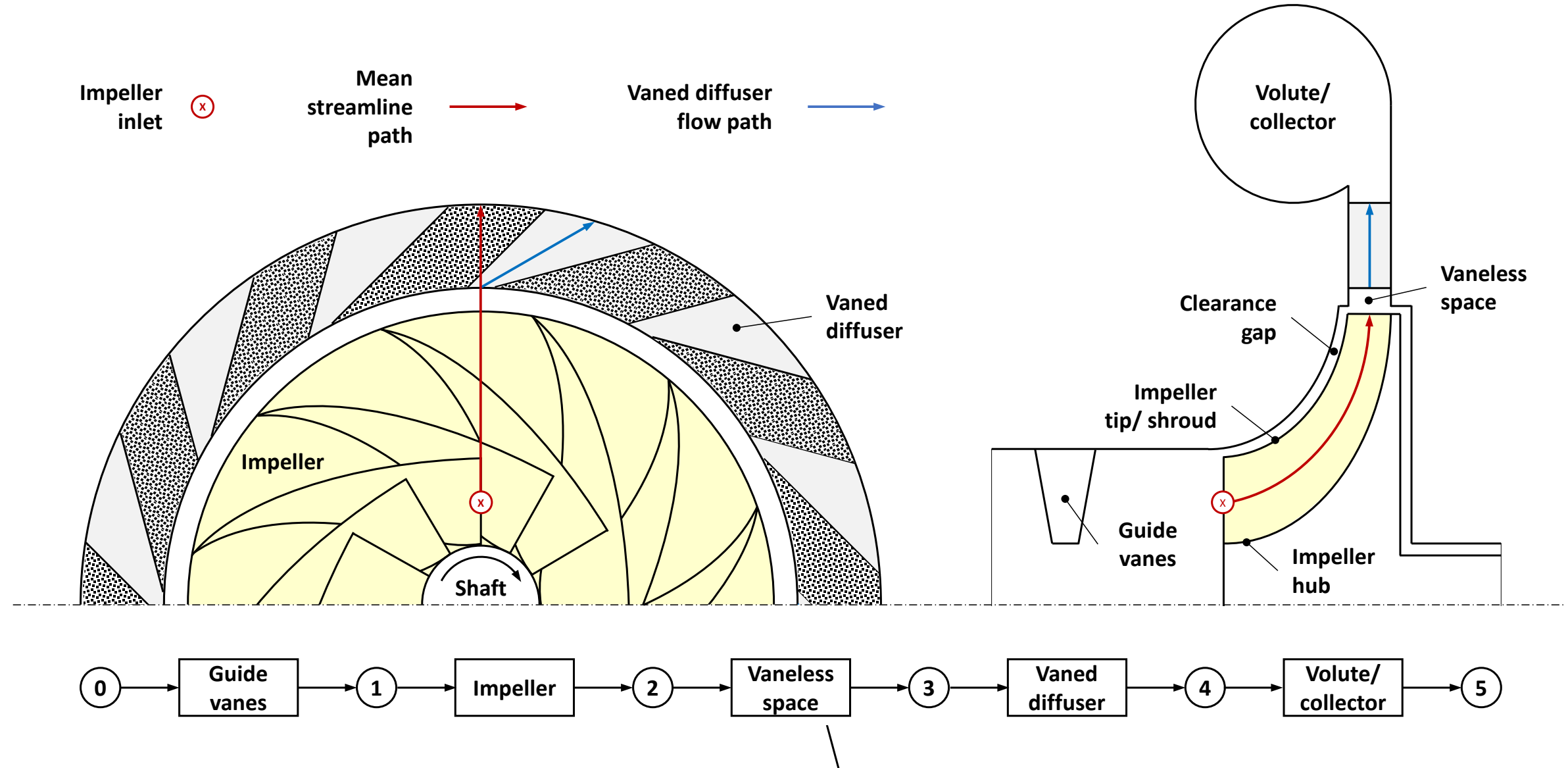


Verification results, from Lee (2016)



Verification results, from Ameli et al. (2018)

Model development



Model verification

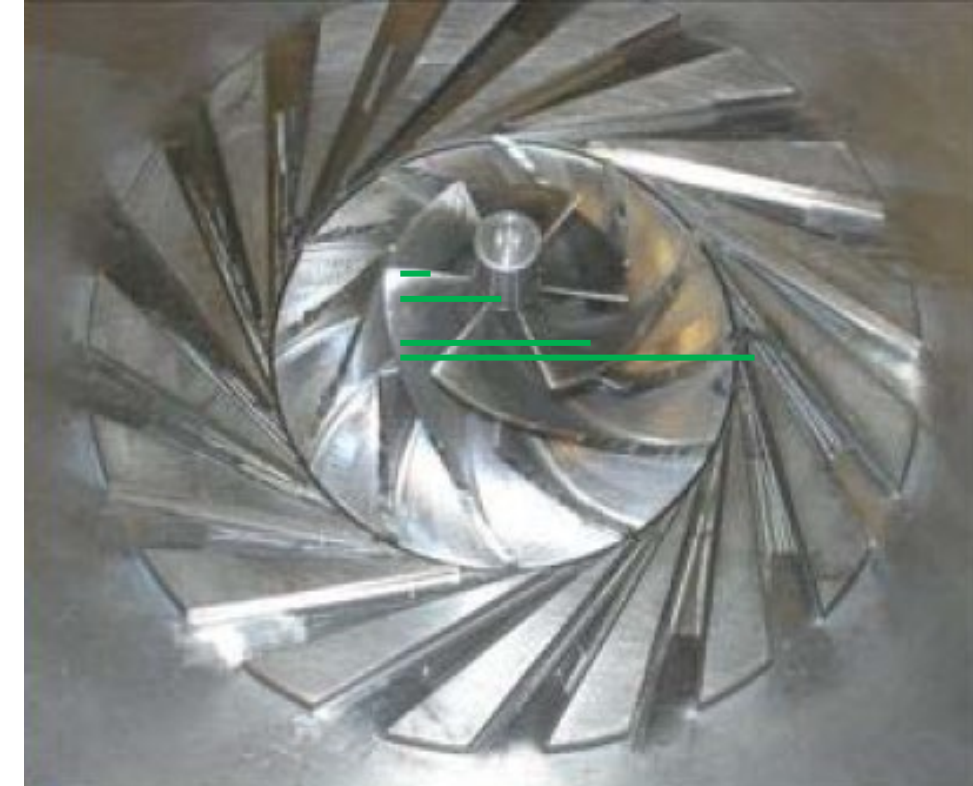
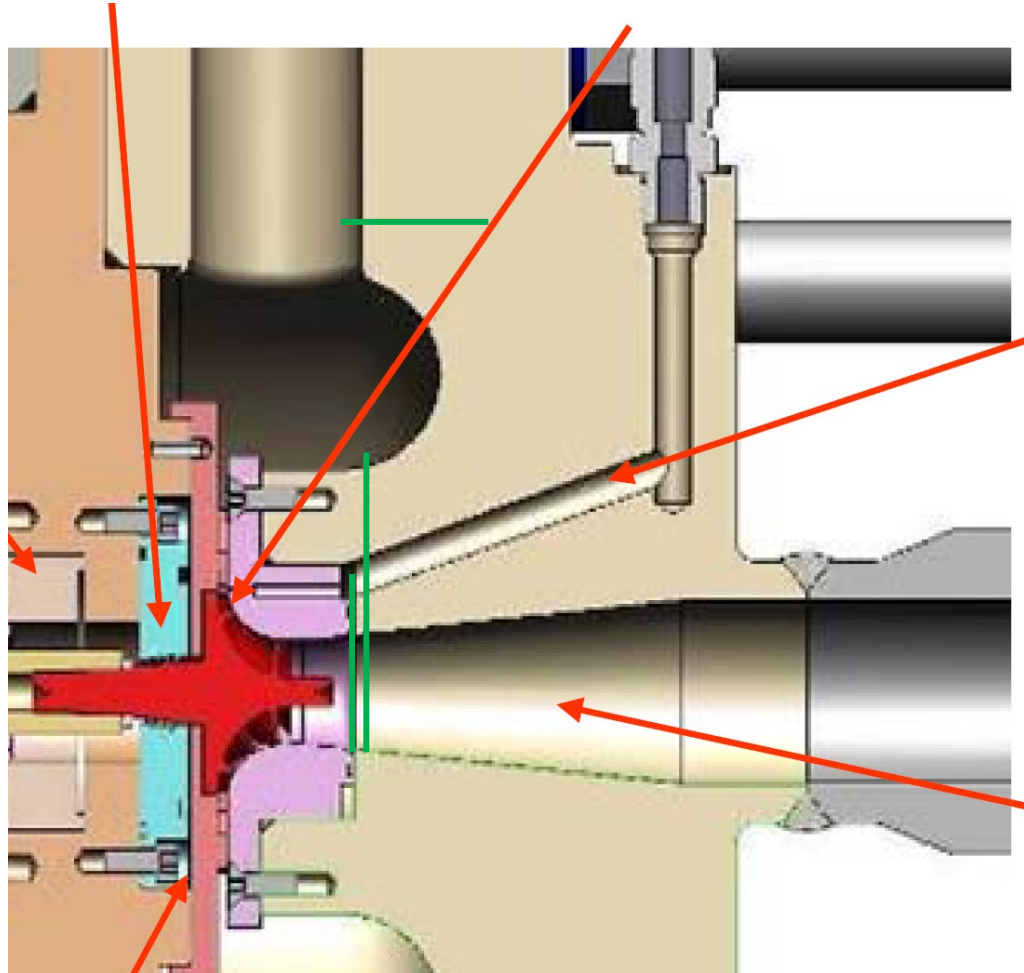


SNL compressor wheel, from Wright et al. (2010)

Model verification

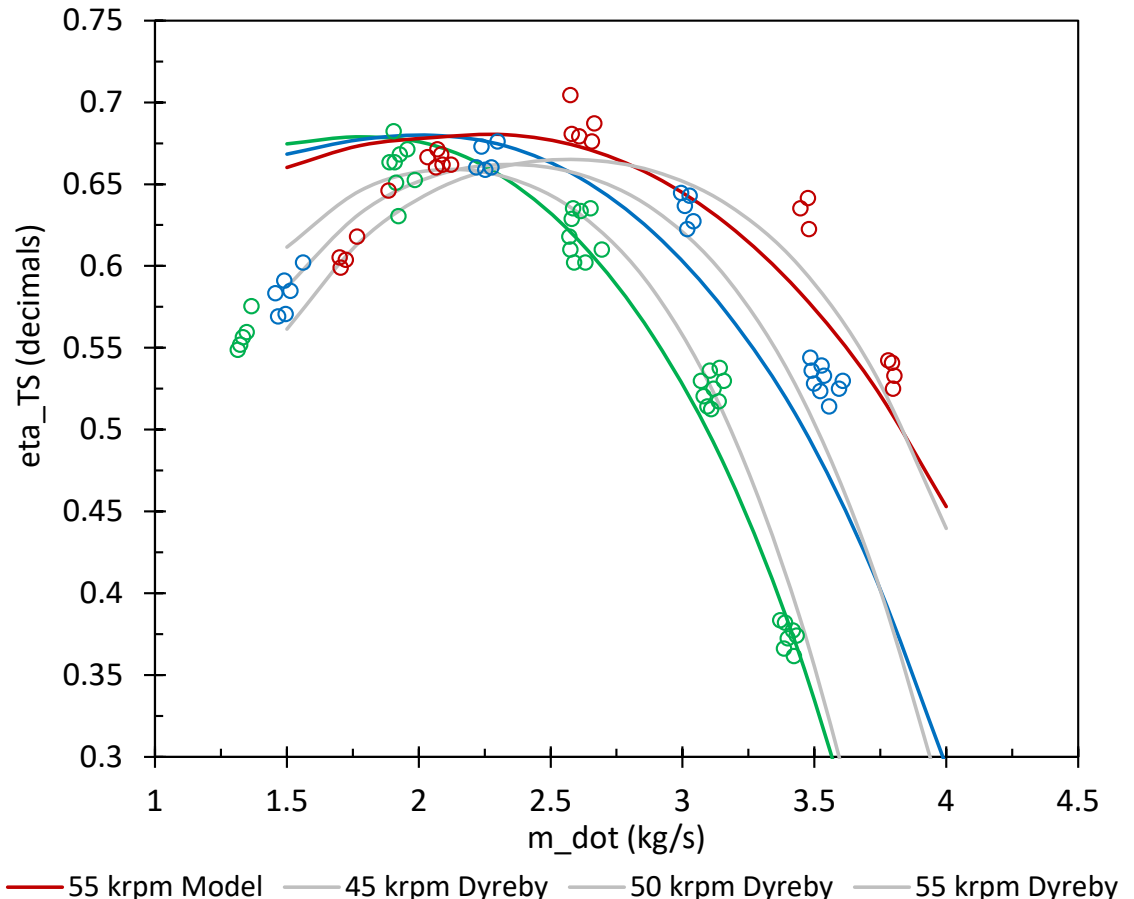
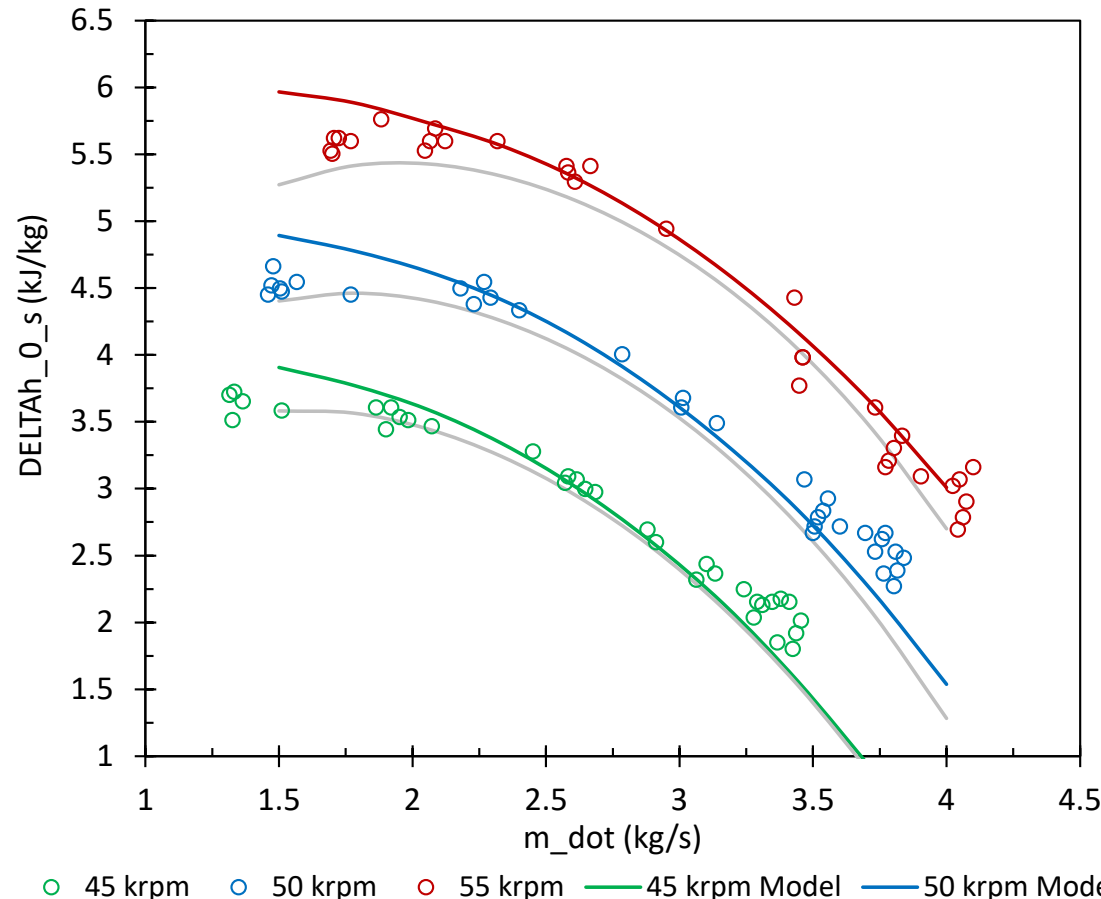
Specification	Units	Value
<i>Known, from Wright et al. (2010)</i>		
Number of full blades	-	6
Number of splitter blades	-	6
Number of vaned diffuser channels	-	17
Blade angle at impeller inlet	°	50.0
Blade angle at impeller exit (backswept)	°	50.0
Vaned diffuser angle at diffuser inlet	°	71.5
Hub radius	mm	2.54
Shroud radius	mm	9.37
Impeller exit radius	mm	18.68
Tip clearance	mm	0.254
Blade thickness	mm	0.76
Blade height at exit	mm	1.71
Nominal mass flow rate	kg/s	3.53
Total pressure at inlet	kPa	7687
Total temperature at inlet	°C	32.15
<i>Assumed</i>		
Ratio of splitter blade to full blade meridional length	-	0.5
Blade angle at impeller inlet (at hub, mean position and shroud)	°	50.0
Vaned diffuser inlet diameter	mm	40
Vaned diffuser exit diameter	mm	75
Vaned diffuser height	mm	1.71
Collector exit diameter	mm	29.89

Model verification



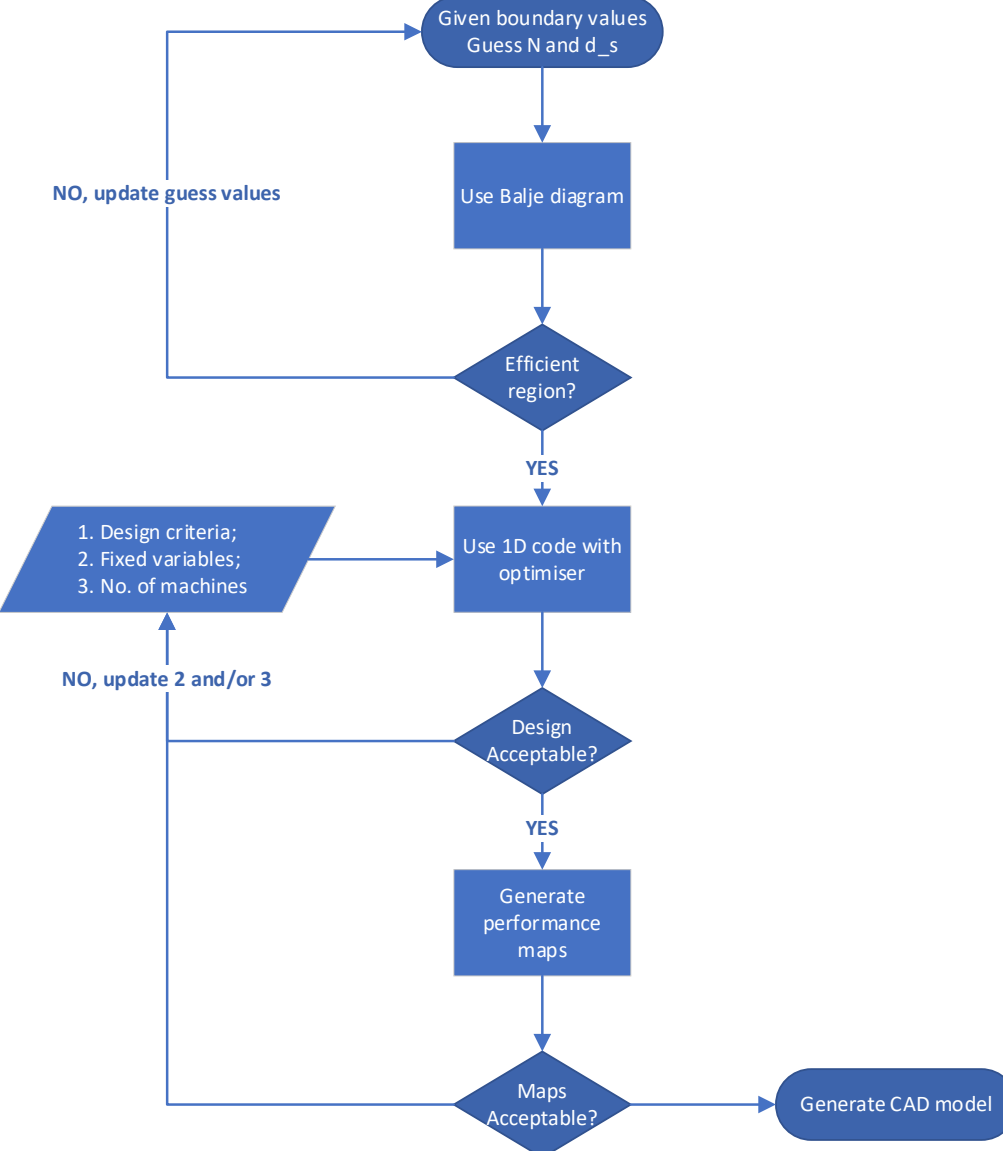
Images of SNL compressor, from Wright et al. (2010)

Model verification

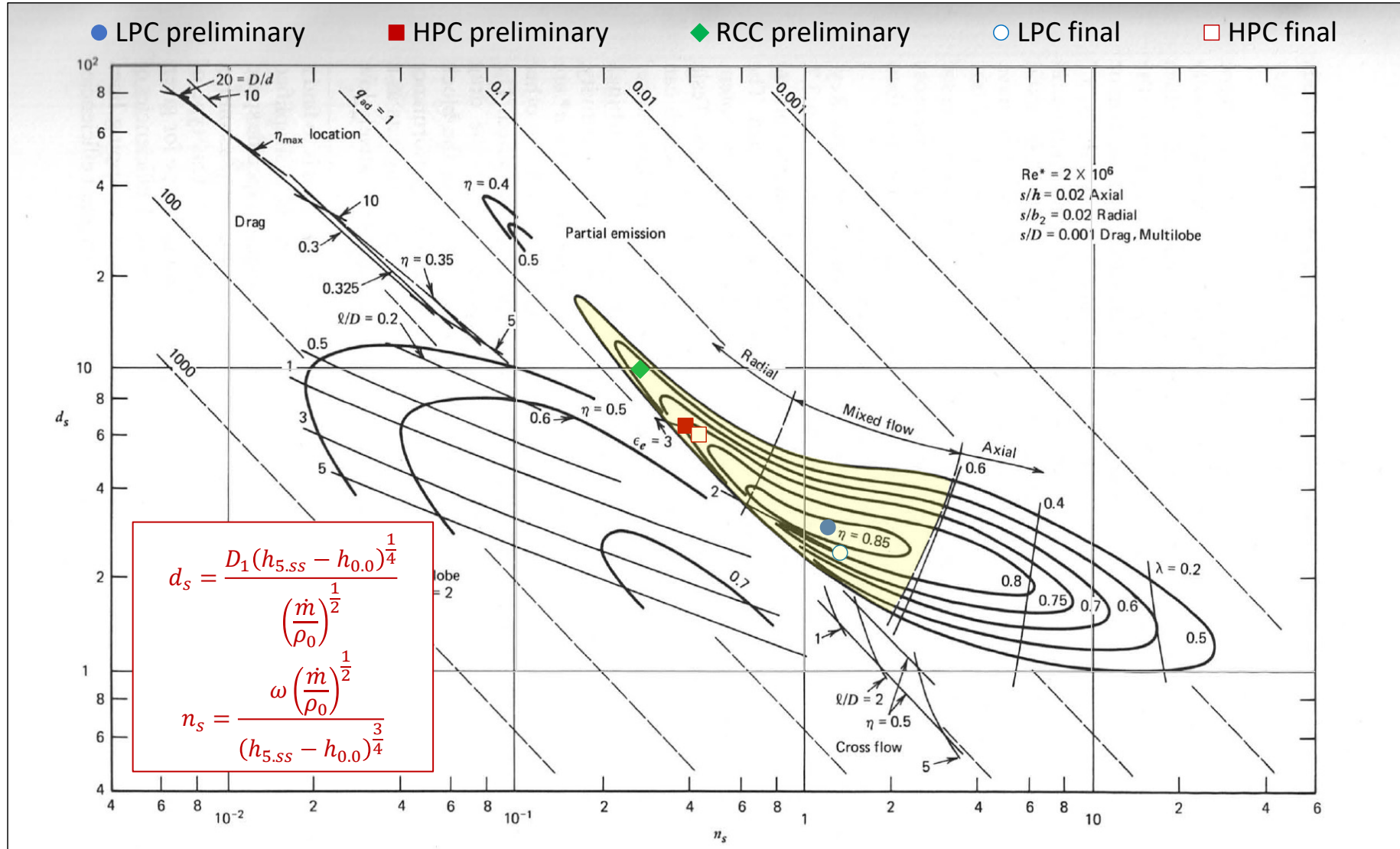


Verification results, test data from Wright et al. (2010)

Sizing method



Initial sizing



Marked up specific diameter-speed diagram, original image from Balje (1981)

1D model inputs

Specification	Units	LPC	HPC
<i>Design criteria</i>			
Mass flow rate	kg/s	397	397
Total pressure at inlet	kPa	7353	9768
Total temperature at inlet	°C	45	45
Total pressure ratio	-	1.356	2.560
Total-to-total efficiency (target)	%	89	89
<i>Fixed variables</i>			
Number of full blades	-	19	19
Number of vane diffuser channels	-	28	28
Nominal design speed	rpm	9000	9000
<i>Optimised variables</i>			
Hub to shroud radius ratio	-	[0.3, 0.6]	
Shroud to tip radius ratio	-	[0.35, 0.65]	
Vane diffuser inlet to impeller exit radius ratio	-	[1.025, 1.075]	
Vane diffuser exit to inlet radius ratio	-	[1.25, 1.75]	
Inlet swirl angle	°	[0, 35]	
Blade angle at impeller inlet (mean position)	°	[25, 50]	
Blade angle at impeller exit (backswept)	°	[25, 50]	

$$OBJECTIVE = X_1 \left(\left| \frac{\eta_{TT} - \eta_{TT.target}}{\eta_{TT.target}} \right| \right) + X_2 \left(\left| \frac{\eta_{TS} - \eta_{TT.target}}{\eta_{TT.target}} \right| \right)$$

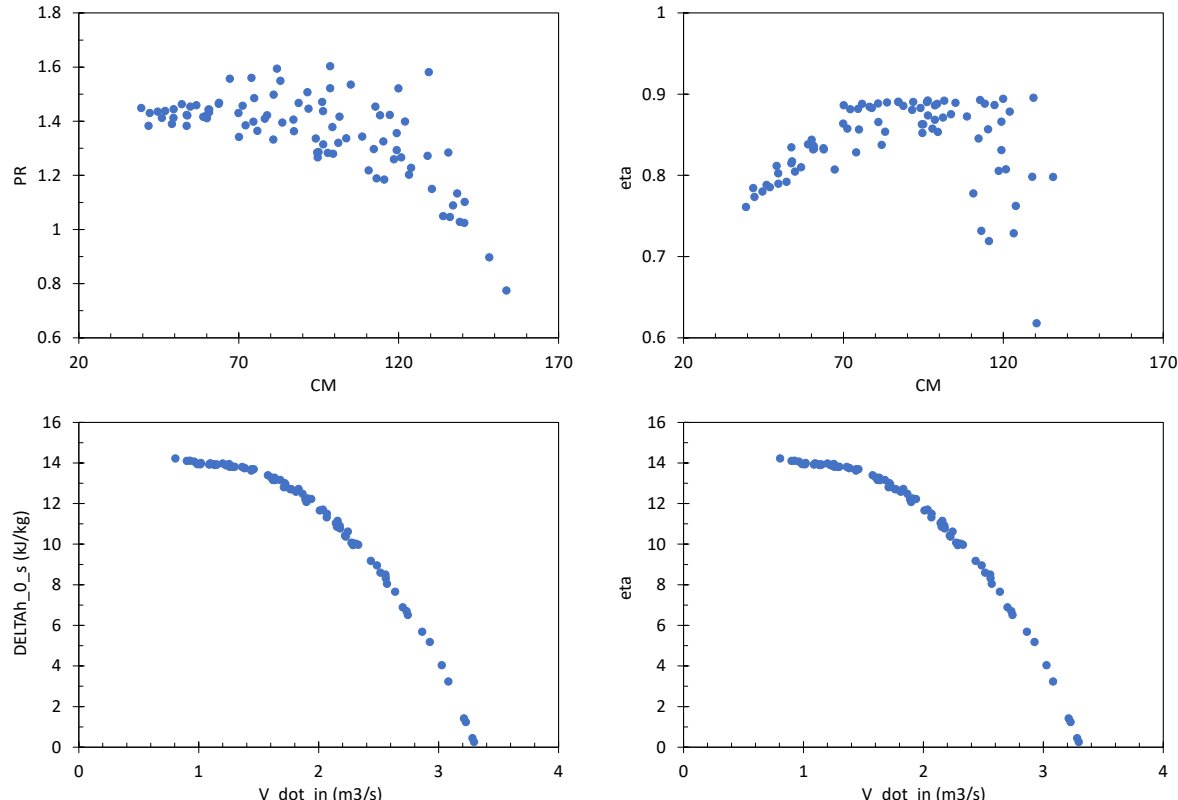
$$X_1 = 0.9; X_2 = 0.1$$

1D model results

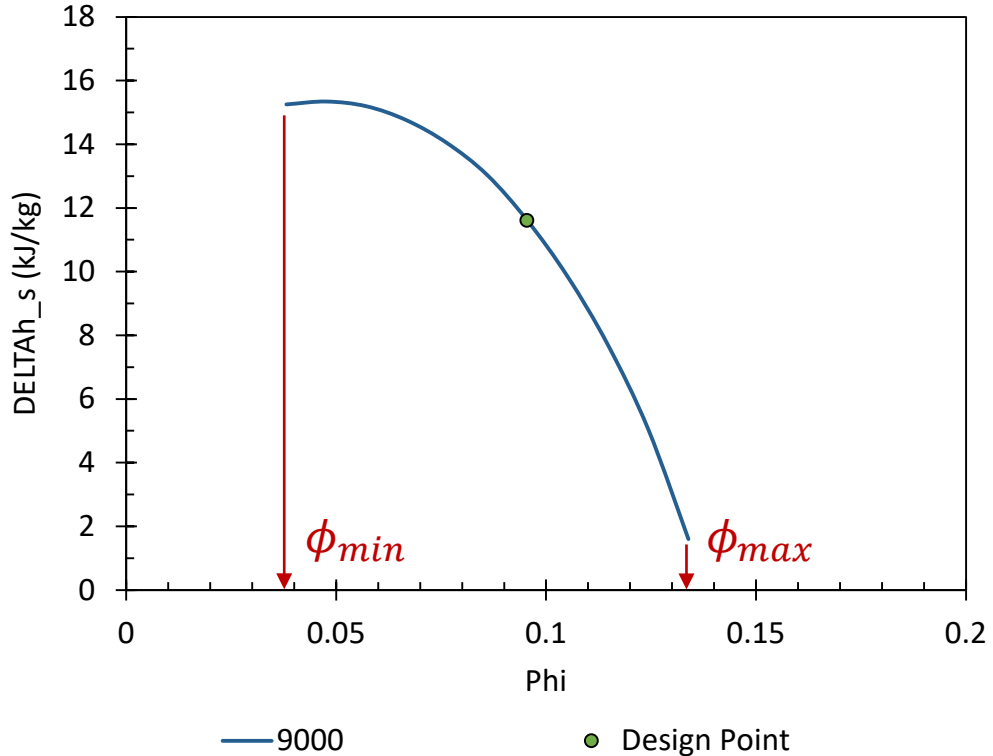
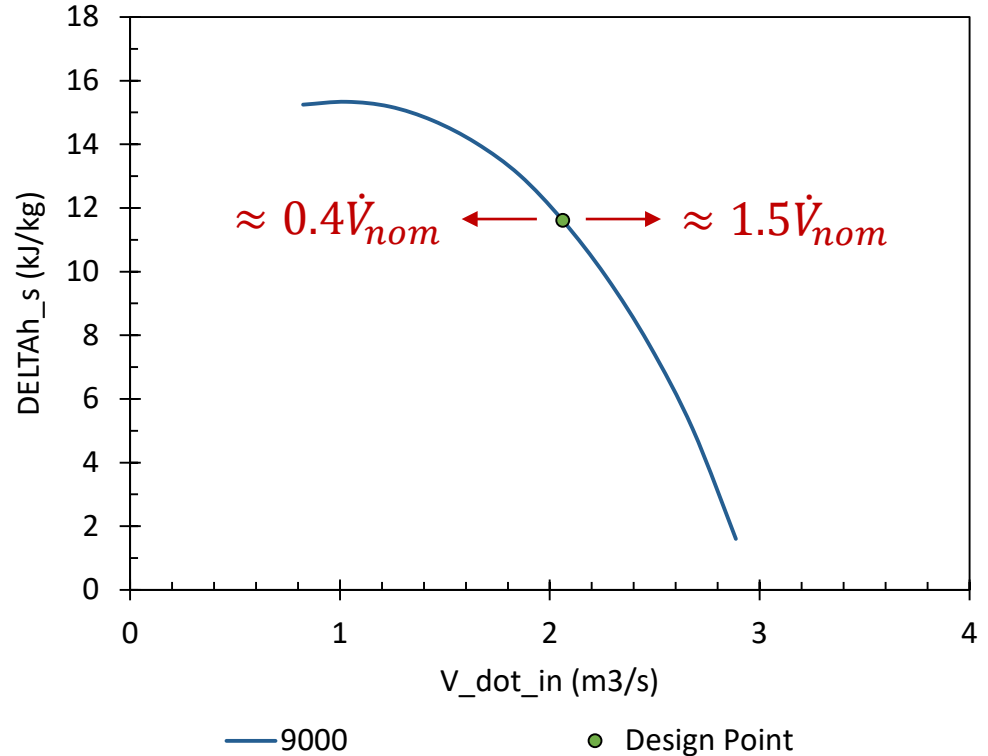
Specification	Units	LPC	HPC
<i>Calculated geometry</i>			
Inlet swirl angle	°	35	17.5
Blade angle at impeller inlet (at hub, mean position and shroud)	°	25.5	37.5
Blade angle at impeller exit (backswept)	°	49.5	37.5
Vaned diffuser mean flow path angle	°	60.5	68.5
Blade height at exit; vaned diffuser height	mm	29.280	8.334
Inlet guide vane upstream diameter	mm	200.7	137.0
Hub diameter	mm	70.0	70.5
Shroud diameter	mm	232.6	157.6
Impeller exit diameter	mm	358.0	450.2
Vaned diffuser inlet diameter	mm	384.9	483.9
Vaned diffuser exit diameter	mm	672.6	846.8
Volute exit diameter	mm	211.3	105.5
Axial length	mm	115.80	91.33
Inertia	kg-mm ²	78 968	181 881
<i>Performance at design point</i>			
Minimum flow coefficient	-	0.0382	0.0084
Maximum flow coefficient	-	0.1339	0.0314
Volume flow rate at inlet	m ³ /s	2.062	0.8986
Isentropic head	kJ/kg	11.61	27.30
Total-to-total efficiency (actual)	%	88.79	89.07
Total-to-static efficiency	%	80.59	80.19
Compressor power	MW	-5.193	-12.166

Performance maps

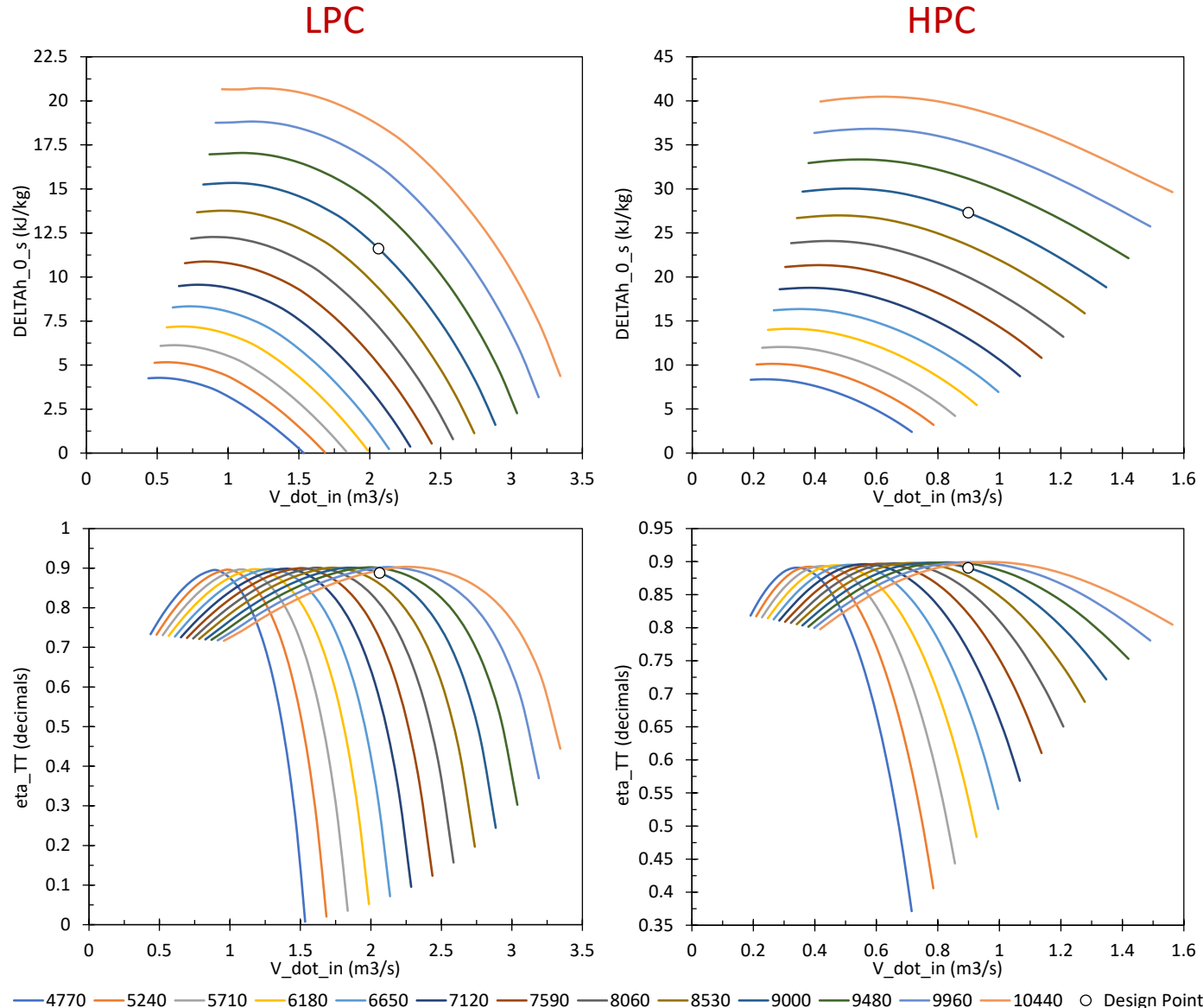
Pressure (kPa)	Temperature (degC)	Mass Flow (kg/s)	PR	eta_TT	CM	CS	DELTAh_0_s (kJ/kg)	eta_TT	Q_dot_in (m ³ /s)	Speed (rpm)
6549.01	38.65	483.80	1.15	0.62	130.40	504.60	5.69	0.64	2.86	9000
7381.07	52.71	556.27	1.05	0.27	136.00	504.60	1.24	0.19	3.23	9000
6649.79	45.57	411.97	1.22	0.78	110.60	504.60	8.05	0.78	2.57	9000
6820.67	49.59	358.89	1.28	0.86	94.52	504.60	10.37	0.86	2.23	9000
8142.50	49.29	541.28	1.29	0.83	119.40	504.60	9.18	0.83	2.44	9000
.
.
.



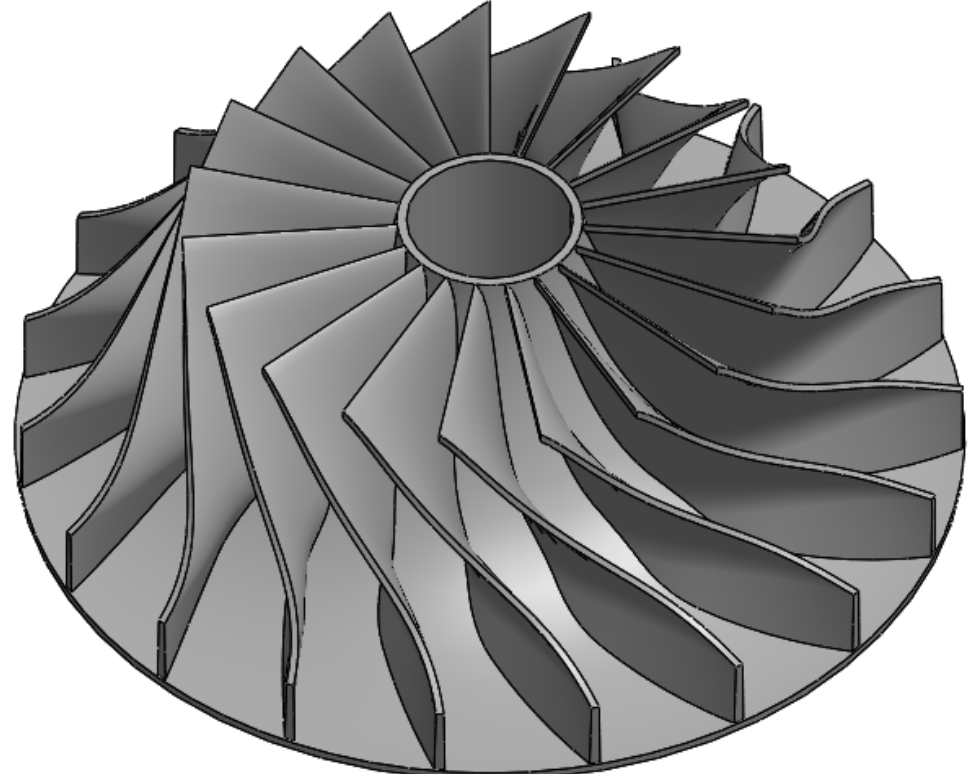
Performance maps



Performance maps

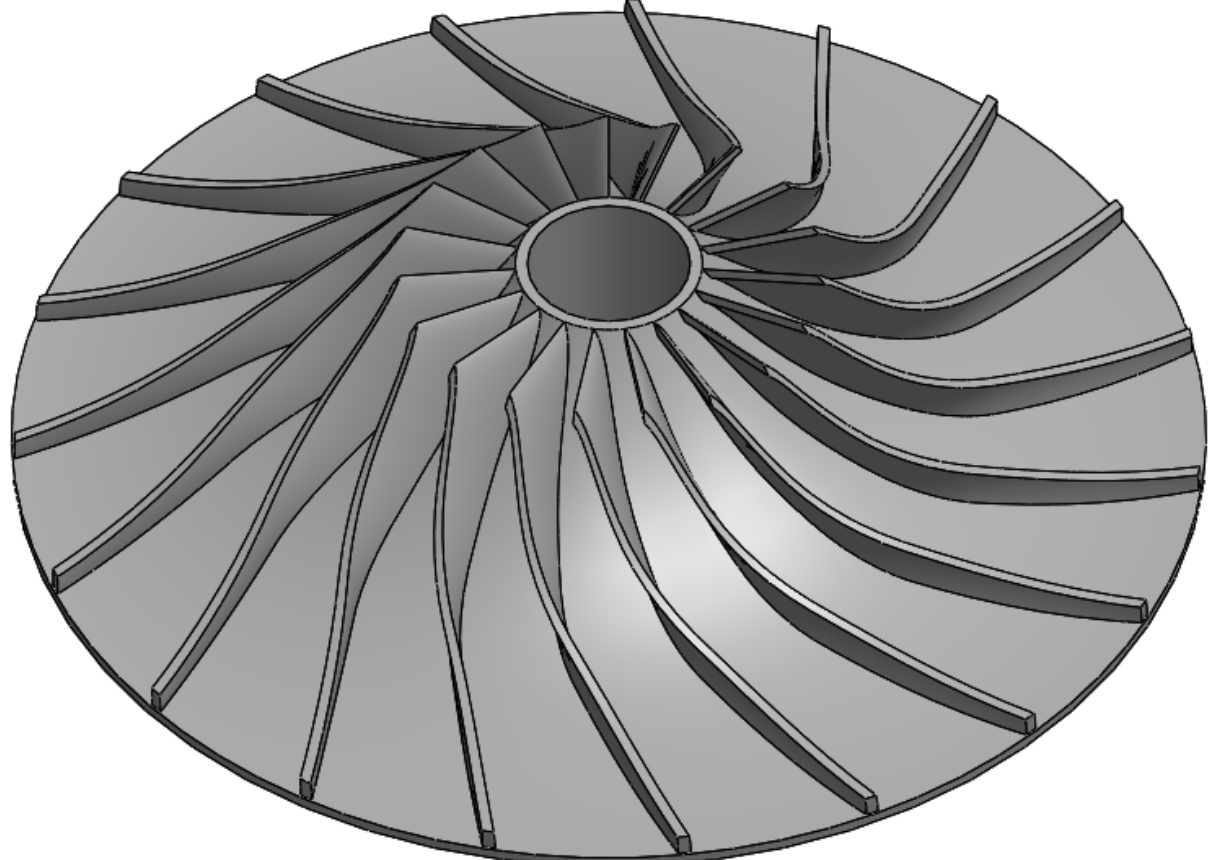


LPC



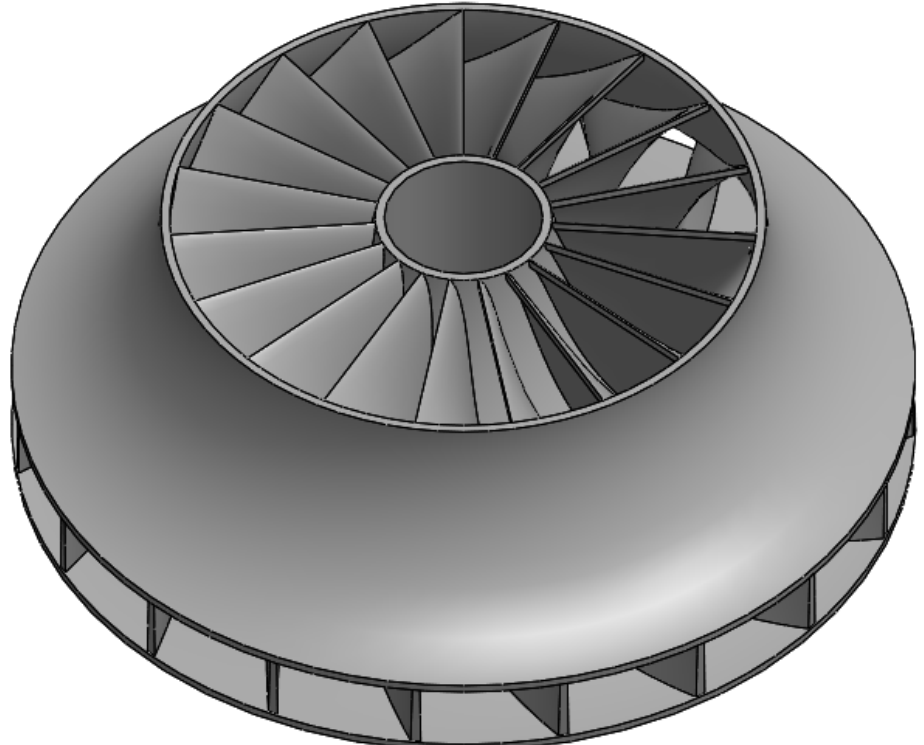
358 x 116

HPC



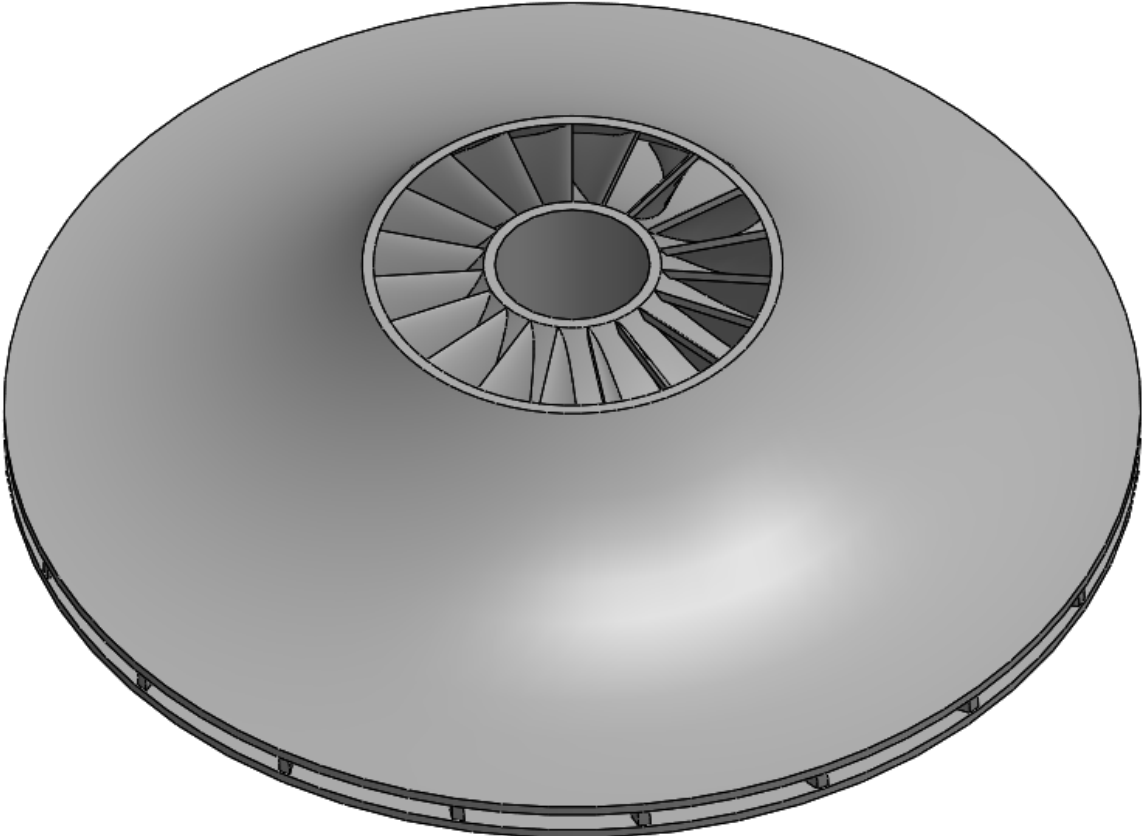
450 x 91

LPC



358 x 116

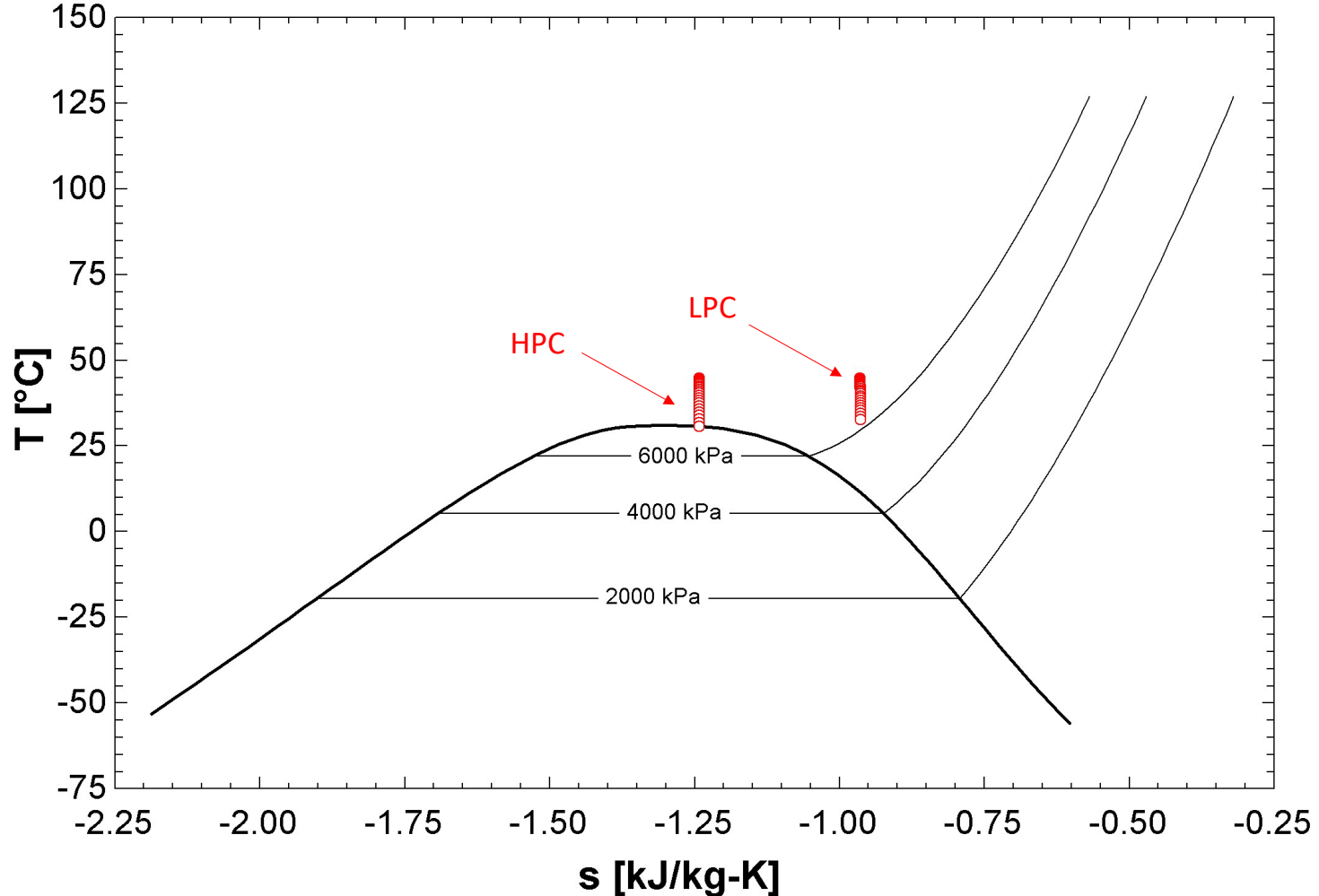
HPC



450 x 91

Minimum static temperatures

For the HPC, when operating at the highest speed and flow rate, a two-phase flow state may be encountered.



Summary and conclusions



- Dynamic compressor models are required for transient simulation studies of sCO₂ cycles.
- Most researchers apply Dyreby's correlations, which is useful, but has shortcomings.
- Except for KAIST-TMD and AlFa CCD, which are not fully documented and leave room for improvement, there are no suitable tools available to size and develop performance maps for sCO₂ radial compressors.

Summary and conclusions

- Dynamic compressor models are required for transient simulation studies of sCO₂ cycles.
- Most researchers apply Dyreby's correlations, which is useful, but has shortcomings.
- Except for KAIST-TMD and AlFa CCD, which are not fully documented and leave room for improvement, there are no suitable tools available to size and develop performance maps for sCO₂ radial compressors.
- In this work:
 - A 1D mean-line code to size centrifugal compressors was developed and verified.
 - The code was used to size centrifugal compressors and develop performance maps.
 - 3D models were developed to estimate the inertia of the compressors.

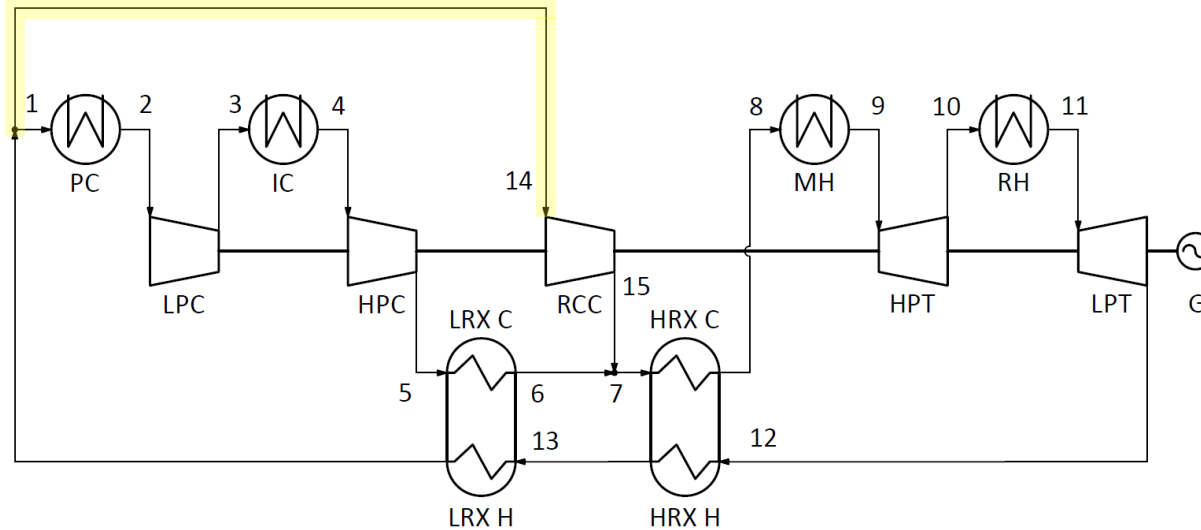
Summary and conclusions

- Dynamic compressor models are required for transient simulation studies of sCO₂ cycles.
- Most researchers apply Dyreby's correlations, which is useful, but has shortcomings.
- Except for KAIST-TMD and AlFa CCD, which are not fully documented and leave room for improvement, there are no suitable tools available to size and develop performance maps for sCO₂ radial compressors.
- In this work:
 - A 1D mean-line code to size centrifugal compressors was developed and verified.
 - The code was used to size centrifugal compressors and develop performance maps.
 - 3D models were developed to estimate the inertia of the compressors.
- The maps and inertia values may be used to model compressors in simulation software.
- The methods employed in this work may be used by others to model centrifugal compressors.

Q&A

Cycles of interest

Partial cooling with reheating cycle



PC: Pre-cooler

IC: Intercooler

LPC: Low pressure compressor

HPC: High pressure compressor

RCC: Recompression compressor

MH: Main heater

RH: Reheater

HPT: High pressure turbine

LPT: Low pressure turbine

LRX: Low temperature recuperator

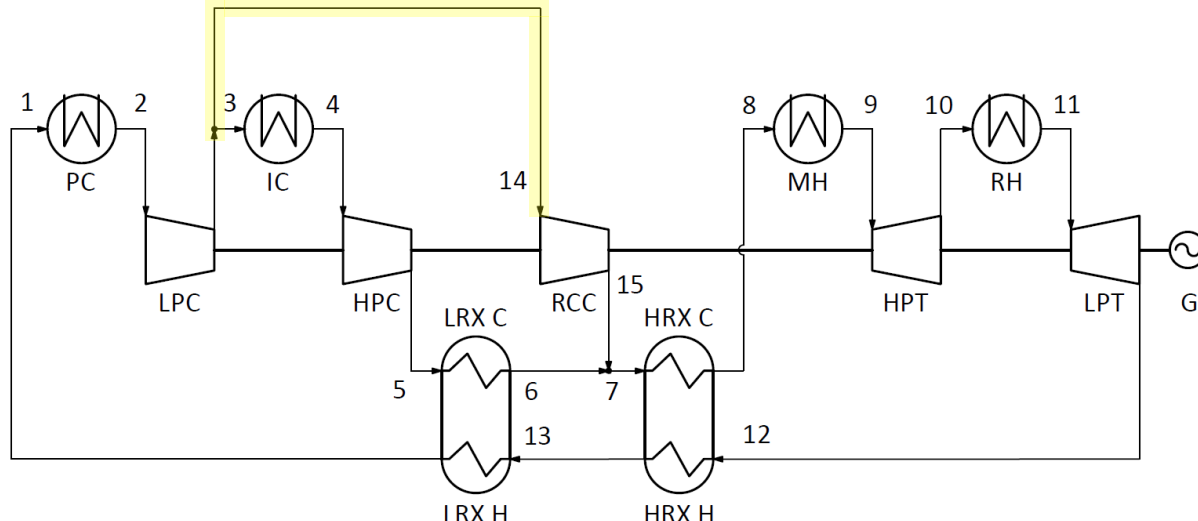
HRX: High temperature recuperator

_C: Cold side

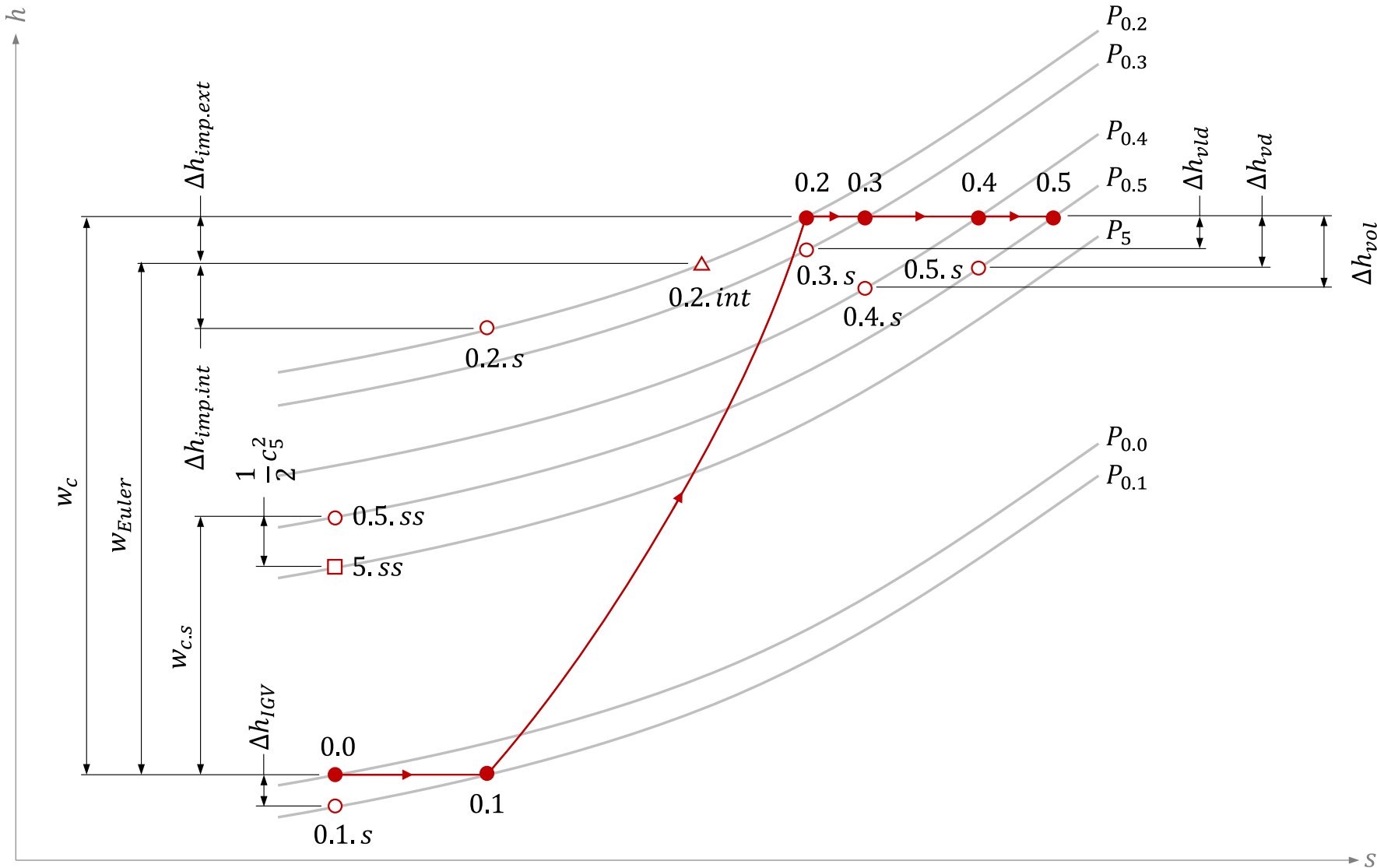
_H: Hot side

G: Generator

Recompression with intercooling and reheating cycle



Mollier diagram



Governing equations



Mass Balance (all elements)

$$\dot{m} = \rho A c$$

Energy Balance (impeller)

$$h_{0.out.s} = h_{0.in} - w_{Euler} - \Delta h_{imp.int}$$

$$h_{0.out} = h_{0.in} - w_{Euler} + \Delta h_{imp.ext}$$

Energy Balance (other elements)

$$h_{0.out.s} = h_{0.in} - \Delta h_{element}$$

$$h_{0.out} = h_{0.in}$$

Entropy Balance (all elements)

$$s_{in} = f(P_{in}, T_{in})$$

$$s_{out.s} = s_{in}$$

$$P_{0.out} = f(h_{0.out.s}, s_{out.s})$$

$$T_{0.out} = f(h_{0.out}, P_{0.out})$$

Governing equations



Real gas fluid property relationships

$$h_0 = h + \frac{1}{2}c^2$$

$$h, \rho, \nu, ss = f(P, T)$$

Work and efficiency definitions

$$w_{c.s} = h_{0.0} - h_{0.5.ss}$$

$$w_c = h_{0.0} - h_{0.5}$$

$$\eta_{TS} = \frac{h_{0.0} - h_{5.ss}}{w_c}$$

$$\eta_{TT} = \frac{w_{c.s}}{w_c}$$

Correlations

Loss/ Model	Source
Inlet guide vanes	(Galvas, 1973)
Internal losses	Skin friction
	Impeller blade loading
	Hub to shroud (for shrouded impellers)
	Mixing
	Clearance (for unshrouded impellers)
	Incidence
	Entrance diffusion
	Choke
	Shock
External losses	Disk friction
	Recirculation
	Leakage (for unshrouded impellers)
Vaneless space (friction)	Based on Jansen (as cited by Ameli et al., 2018)
Vaned diffuser (incidence)	Aungier (as cited by Zhang et al., 2019)
Vaned diffuser (friction)	Based on Jansen (as cited by Ameli et al., 2018)
Volute pressure recovery	Japikse & Baines (1997)
Slip factor	Wiesner (1967)

Software



Related work

- Steady state cycle study:
 - du Sart, C.F., Rousseau, P. & Laubscher, R. 2024. Comparing the partial cooling and recompression cycles for a 50 MWe sCO₂ CSP plant using detailed recuperator models. *Renewable Energy*. DOI: 10.1016/j.renene.2024.119980.
- Solar field and receiver studies:
 - Heydenrych, J.M., Rousseau, P.G. & du Sart, C.F. 2022. Reduced-order modelling of central solar tower receivers using an equivalent thermal resistance network. In *Proceedings of the 16th international conference on heat transfer, fluid mechanics and thermodynamics (HEFAT-16)*. Virtual: HEFAT. 911–916. Available: <https://www.researchgate.net/publication/363173202>.
 - Heydenrych, J.M., Rousseau, P.G. & du Sart, C.F. 2023. A reduced order modelling methodology for concentrated solar power external cylindrical receivers. In *Proceedings of the 17th international heat transfer conference (IHTC-17)*. Cape Town: Begell House. Available: <https://ihtcdigitallibrary.com/conferences/ihtc17,7188217e24389634,15e3d1eb26dcb54a.html>.
- Heat rejection system study:
 - Abrahams, L., du Sart, C. & Laubscher, R. 2022. Design of an air-cooled heat rejection system for a SC0₂ concentrated solar power plant. In *16th international conference on heat transfer, fluid mechanics and thermodynamics (HEFAT-16)*. Virtual: HEFAT. 288–293. Available: <https://www.researchgate.net/publication/363173234>.
- Turbine studies:
 - du Sart, C.F., Rousseau, P. & Laubscher, R. 2024. A method to develop centrifugal turbine performance maps for off-design and dynamic simulation studies of sCO₂ cycles. In Review.
 - Laubscher, R., Rousseau, P., Van Der Spuy, J., du Sart, C. & Johannes, P. A unified thermofluid network simulation methodology to model centrifugal compressors with supercritical real gas working fluids. In Review.

References

- Ameli, A., Turunen-saaresti, T., Grönman, A. & Backman, J. 2018. Compressor design method in the supercritical CO₂ applications. The 6th International Symposium - Supercritical CO₂ Power Cycles.
- Aungier, R.H. 1995. Mean streamline aerodynamic performance analysis of centrifugal compressors. *Journal of Turbomachinery*. 117(3):360–366. DOI: 10.1115/1.2835669.
- Aungier, R.H. 2000. Centrifugal Compressors: A Strategy for Aerodynamic Design and Analysis. New York: ASME Press. DOI: 10.1115/1.800938.
- Balje, O.E. 1981. Turbomachines: A Guide to Design, Selection, and Theory. New York: John Wiley & Sons.
- Binotti, M., Astolfi, M., Campanari, S., Manzolini, G. & Silva, P. 2017. Preliminary assessment of sCO₂ cycles for power generation in CSP solar tower plants. *Applied Energy*. 204:1007–1017. DOI: 10.1016/j.apenergy.2017.05.121.
- Carstens, N. 2007. Control strategies for supercritical carbon dioxide power conversion systems. Massachusetts Institute of Technology.
- Cho, S.K., Bae, S.J., Jeong, Y., Lee, J. & Lee, J.I. 2019. Direction for high-performance supercritical CO₂ centrifugal compressor design for dry cooled supercritical CO₂ Brayton cycle. *Applied Sciences (Switzerland)*. 9(19). DOI: 10.3390/app9194057.
- Correa, F., Barraza, R., Soo Too, Y.C., Vasquez Padilla, R. & Cardemil, J.M. 2021. Optimized operation of recompression sCO₂ Brayton cycle based on adjustable recompression fraction under variable conditions. *Energy*. 227. DOI: 10.1016/j.energy.2021.120334.
- Dostal, V., Driscoll, M.J. & Hejzlar, P. 2004. A Supercritical Carbon Dioxide Cycle for Next Generation Nuclear Reactors. Massachusetts Institute of Technology.
- Dyreby, J.J. 2014. Modeling the Supercritical Carbon Dioxide Brayton Cycle with Recompression. WISCONSIN-MADISON.
- Flownex SE. 2020. Flownex Library Manual.
- Galvas, M. 1973. Fortran program for predicting off-design performance of centrifugal compressors. Washington DC.
- Harrison, H.M. 2020. Development and Validation of a New Method To Model Slip and Work Input for Centrifugal Compressors. Purdue University.
- Japikse, D. & Baines, N.C. 1997. Introduction to Turbomachinery. Concepts ETI Inc. and Oxford University Press.
- Jeong, Y., Son, S., Cho, S.K., Baik, S. & Lee, J.I. 2020. Evaluation of supercritical CO₂ compressor off-design performance prediction methods. *Energy*. 213:119071. DOI: 10.1016/j.energy.2020.119071.
- Kulhanek, M. & Dostal, V. 2011. Thermodynamic Analysis and Comparison of Supercritical Carbon Dioxide Cycles. In Supercritical CO₂ Power Cycle Symposium. Boulder.

References

- Lee, J. 2016. Study of improved design methodology of S-CO₂ power cycle compressor for the next generation nuclear system application. Korea Advanced Institute of Science and Technology. Available: <https://kdrm.kaist.ac.kr/ezpdfwebviewer/ezpdf/customLayout.jsp?encdata=67D4CD8135C7372A42DB0940C33C3EA11F56B0C612D0A8D3799BF481C377949DE464993BE0419278598BD59B7D4A0373654623C1456D6BC18194BAD1257817965B00F5FD41B0997C&lang=ko#>.
- Luu, M.T., Milani, D., McNaughton, R. & Abbas, A. 2017a. Analysis for flexible operation of supercritical CO₂ Brayton cycle integrated with solar thermal systems. *Energy*. 124:752–771. DOI: 10.1016/j.energy.2017.02.040.
- Luu, M.T., Milani, D., McNaughton, R. & Abbas, A. 2017b. Dynamic modelling and start-up operation of a solar-assisted recompression supercritical CO₂ Brayton power cycle. *Applied Energy*. 199:247–263. DOI: 10.1016/j.apenergy.2017.04.073.
- Mehos, M., Turchi, C., Vidal, J., Wagner, M., Ma, Z., Ho, C., Kolb, W., Andraka, C., et al. 2017. Concentrating Solar Power Gen3 Demonstration Roadmap. Available: <https://www.nrel.gov/docs/fy17osti/67464.pdf>.
- Neises, T. & Turchi, C.S. 2014. A comparison of supercritical carbon dioxide power cycle configurations with an emphasis on CSP applications. *Energy Procedia*. 49:1187–1196. DOI: 10.1016/j.egypro.2014.03.128.
- Neises, T. & Turchi, C.S. 2019. Supercritical carbon dioxide power cycle design and configuration optimization to minimize levelized cost of energy of molten salt power towers operating at 650 °C. *Solar Energy*. 181(November 2018):27–36. DOI: 10.1016/j.solener.2019.01.078.
- Oh, H.W., Yoon, E.S. & Chung, M.K. 1997. An optimum set of loss models for performance prediction of centrifugal compressors. *Proceedings of the Institution of Mechanical Engineers, Part A: Journal of Power and Energy*. 211:331–338. DOI: 10.1243/0957650971537231.
- Osorio, J.D., Hovsepian, R. & Ordonez, J.C. 2016. Dynamic analysis of concentrated solar supercritical CO₂-based power generation closed-loop cycle. *Applied Thermal Engineering*. 93:920–934. DOI: 10.1016/j.aplthermaleng.2015.10.039.
- Padilla, R.V., Benito, R.G. & Stein, W. 2015. An Exergy Analysis of Recompression Supercritical CO₂ Cycles with and without Reheating. *Energy Procedia*. 69:1181–1191. DOI: 10.1016/j.egypro.2015.03.201.
- Seidel, W. 2010. Model development and annual simulation of the supercritical carbon dioxide Brayton cycle for concentrating solar power applications. University of Wisconsin - Madison.
- Thanganadar, D., Fornarelli, F., Camporeale, S., Asfand, F. & Patchigolla, K. 2020. Analysis of design, off-design and annual performance of supercritical CO₂ cycles for csp applications. *Proceedings of the ASME Turbo Expo*. 11:1–9. DOI: 10.1115/GT2020-14790.
- The World Bank. 2019. Global Solar Atlas. Available: <https://globalsolaratlas.info/download> [2020, September 04].

References

- Turchi, C.S., Ma, Z., Neises, T.W. & Wagner, M.J. 2013. Thermodynamic study of advanced supercritical carbon dioxide power cycles for concentrating solar power systems. *Journal of Solar Energy Engineering, Transactions of the ASME.* 135(4):1–7. DOI: 10.1115/1.4024030.
- Wiesner, F.J. 1967. A review of slip factors for centrifugal impellers. *Journal of Engineering for Gas Turbines and Power.* 89(4):558–566. DOI: 10.1115/1.3616734.
- Wright, S.A., Radel, R.F., Vernon, M.E., Rochau, G.E. & Pickard, P.S. 2010. Operation and Analysis of a Supercritical CO₂ Brayton Cycle. Albuquerque. DOI: <https://doi.org/10.2172/984129>.
- Yang, J., Yang, Z. & Duan, Y. 2023. Design Optimization and Operating Performance of S-CO₂ Brayton Cycle under Fluctuating Ambient Temperature and Diverse Power Demand Scenarios. *Journal of Thermal Science.* 32. DOI: 10.1007/s11630-023-1839-2.